AD NUMBER

AD475564

LIMITATION CHANGES

TO:

Approved for public release; distribution is unlimited.

FROM:

Distribution authorized to U.S. Gov't. agencies and their contractors; Critical Technology; DEC 1965. Other requests shall be referred to Air Force Arnold Engineering Development Center, Rocket Test Facility, Arnold AFB, TN. This document contains export-controlled technical data.

AUTHORITY

aedc usae ltr 24 feb 1972

AEDC-TR-65-250

C. E. Robinson

THRUST VECTOR DETERMINATION FOR THE APOLLO SERVICE PROPULSION ENGINE USING A SIX-COMPONENT FORCE BALANCE

C. E. Robinson and R. B. Runyan

ARO, Inc.

December 1965

ROCKET TEST FACILITY
ARNOLD ENGINEERING DEVELOPMENT CENTER
AIR FORCE SYSTEMS COMMAND
ARNOLD AIR FORCE STATION, TENNESSEE

NOTICES

When U. S. Government drawings specifications, or other data are used for any purpose other than a definitely related Government procurement operation, the Government thereby incurs no responsibility nor any obligation whatsoever, and the fact that the Government may have formulated, furnished, or in any way supplied the said drawings, specifications, or other data, is not to be regarded by implication or otherwise, or in any manner licensing the holder or any other person or corporation, or conveying any rights or permission to manufacture, use, or sell any patented invention that may in any way be related thereto.

Qualified users may obtain copies of this report from the Defense Documentation Center.

References to named commercial products in this report are not to be considered in any sense as an endorsement of the product by the United States Air Force or the Government.

THRUST VECTOR DETERMINATION FOR THE APOLLO SERVICE PROPULSION ENGINE USING A SIX-COMPONENT FORCE BALANCE

C. E. Robinson and R. B. Runyan
ARO, Inc.

FOREWORD

This report contains the test results obtained on a multicomponent force system developed to determine thrust vector excursions of the Apollo Service Module (S/M) engine (AJ10-137) under System 921E. The Apollo S/M engine program is sponsored by the National Aeronautics and Space Administration, Manned Spacecraft Center (NASA-MSC). Technical liaison was provided by the Aerojet-General Corporation (AGC), subcontractor of the Apollo S/M engine, and North American Aviation, Space and Information Systems Division (NAA-S&ID), prime contractor for the S/M.

The multicomponent force system was developed by ARO, Inc. (a subsidiary of Sverdrup and Parcel, Inc.), Arnold Engineering Development Center (AEDC), Air Force Systems Command (AFSC), under Contract AF 40(600)-1200. The results reported herein were obtained in the Propulsion Engine Test Cell (J-3) during the period between September 1, 1964, and July 11, 1965, under ARO Project No. RM1356, and the manuscript was submitted for publication on November 4, 1965.

The authors are grateful to D. Gray, Jr., and C. K. Acker (Scientific Computing Service) for writing the computer program for data reduction and to D. K. Graham, J. C. Blevins, W. E. Spenglar, and Flora T. Yando (Propulsion Wind Tunnel Facility) for the use of their previous work on six-component wind tunnel force strain-gage balances.

This technical report has been reviewed and is approved.

Ralph W. Everett
Major, USAF
AF Representative, RTF
DCS/Test

Jean A. Jack
Colonel, USAF
DCS/Test

ABSTRACT

A multicomponent force system was developed to determine the line of action of the forces generated by the Apollo Service Module engine. This force system was a force balance based on the principles of linear and repeatable installation tare effects. The basic concepts of the force balance and the statistical accuracies which were achieved are presented along with a detailed discussion of the calibration procedure and data reduction methods. Thrust vector excursion for two ablative combustion chambers during nongimbaling engine operation and limited thrust vector data during gimbaling operation are also presented. The precision of the thrust vector data was determined to be 0.033 deg for angular measurement and 0.026 in. for position determination.

CONTENTS

ILLUSTRATIONS

TABLES

NOMENCLATURE

C	Calibration constant, lb_f/lb_f
$\frac{dS}{dX}$	Slope of data load cell output versus applied load as a function of load application position, $lb_f/in.\text{-}lb_f$
F_a	Axial force, lb_f
F_{P_1}	Pitch force, forward, lb_f

F_{P_2}	Pitch force, aft, lb_f
F_R	Roll force, lb_f
F_{Y_1}	Yaw force, forward, lb_f
F_{Y_2}	Yaw force, aft, lb_f
K	Intercept of dS/dX
k	Balance constants, lb_f/lb_f
L	Actual force applied, lb_f
L_{P_1}	Forward pitch load cell
L_{P_2}	Aft pitch load cell
M	Moment
M_p	Total pitching moment, in.-lb
M_r	Total rolling moment, in.-lb
M_y	Total yawing moment, in.-lb
R	Data load cell output, lb_f
S	Slope of data load cell output versus applied load, lb_f/lb_f
X_1	Distance from electrical center of forward pitch load cell to engine gimbal plane, in.
X_2	Distance from electrical center of aft pitch load cell to engine gimbal plane, in.
X_3	Distance from roll data load cell to engine gimbal plane, in.
X_P	Distance from reference plane to midpoint of electrical centers, pitch plane, in.
X_{PF}	Location of applied pitch force
ΔX_P	Distance between electrical centers for forward and aft pitch load cells, in.
X_Y	Distance from reference plane to midpoint of electrical centers, yaw plane, in.
ΔX_Y	Distance between electrical centers for forward and aft yaw load cells, in.
Y_1	Distance from electrical center of forward yaw load cell to engine gimbal plane, in.
Y_2	Distance from electrical center of aft yaw load cell to engine gimbal plane, in.

Z_1	Distance from roll data load cell to balance centerline, in.
η	Location of point of thrust vector intersection with engine gimbal plane on yaw axis, in.
θ	Thrust vector deviation from vertical in pitch plane, deg
ξ	Location of point of thrust vector intersection with engine gimbal plane on pitch axis, in.
ϕ	Thrust vector deviation from vertical in yaw plane, deg

SUBSCRIPTS

cal	Calibrate
data	Data
i	Data load cell being considered, varies from 1 to 6
j	Calibrate load cell being considered, varies from 1 to 6
p	Pitch
t	Total
y	Yaw
z	Loading plane designation

SECTION I
INTRODUCTION

With the advent of ablatively cooled liquid-propellant combustion chambers, the need for determining the thermal and ablation effects on the thrust vector position became a prominent concern of engine manufacturers. These effects will not necessarily follow a similar pattern for any two combustion chambers. Therefore, to form a basis for predicting the thrust vector excursion due to the thermal and ablation effects, experimental data on several chambers are necessary. To provide thrust vector position with respect to burn time requires the use of a multicomponent force measuring system. Careful consideration of the force system alignment and of the engine alignment within the force system must be observed to define the exact location of the generated thrust.

A six-component force system was designed for use in determining the ablative and thermal effects on the line of action of thrust for the Aerojet-General Corporation (AGC) AJ10-137 Apollo Service Module (S/M) engine during tests conducted at simulated altitude conditions in the Propulsion Engine Test Cell (J-3). This force balance system was designed for linear and repeatable installation tare effects so that linear corrections could be made to the measured component forces to obtain the actual applied forces.

This report presents a description of the J-3 force balance, the method of calibration of the balance, calibration evaluation techniques, an error analysis for the force balance, and the thrust vector data obtained during testing of the AJ10-137 engine.

SECTION II
APPARATUS

2.1 INSTALLATION

A multicomponent force system was employed to measure the forces generated by the AJ10-137 engine. The following six-components of force were measured: (1) axial force, (2) forward pitch, (3) aft pitch, (4) roll, (5) forward yaw, and (6) aft yaw. These components are shown schematically in Fig. 1a.

The multicomponent force system is installed vertically in the Propulsion Engine Test Cell (J-3)[1] as shown in Fig. 1b. The force system is composed of an outer cage and an inner cage. The inner cage receives forces applied by the engine through two engine mounting pads (Fig. 1c) and a yaw actuator attachment point. All forces are transmitted by the inner cage through data load trains containing force measuring load cells which are isolated by universal flexures from the cell ground system. The outer cage is the ground for side force measurements and is rigidly connected to the test cell ground (Fig. 1b). The inner and outer thrust cages are constructed for maximum rigidity under expected side forces.

For each force measuring load cell, there is a corresponding calibrate load cell (Fig. 2). The calibrate loads for pitch, yaw, and roll are applied with pneumatic loaders that apply both tension and compression loads to the data load cell. Gaseous nitrogen is used to apply pressure to the loader. Each pneumatic loader has a spring which returns the piston to null under a no-pressure condition. Axial calibrate loads are applied with a hydraulic loader. The calibrate load trains are disconnected from the system during engine firings. Figure 3 presents some photographs of the load train installation.

2.2 INSTRUMENTATION

All force measuring load cells are dual-output strain-gage-type cells. The axial load cell has a capacity of 50,000 lb_f. The side force cells, both pitch and yaw, and the roll load cell are 500 lb_f for both the data and calibrate systems.

The outputs of the force data and calibrate load cells were recorded by three systems during calibrations. The forces were recorded on a light-beam oscillograph for immediate control room observation, on a magnetic tape analog-to-digital system for on-line engineering data in the control room, and on an analog-to-frequency high resolution magnetic tape system for high-speed computer reduction. The calibration data from the analog-to-frequency magnetic tape system were used in determining the balance constants. During engine firings, the analog-to-frequency recording system was used to record data for thrust vector determination.

---

[1] Test Facilities Handbook (5th Edition). "Rocket Test Facility, Vol. 2." Arnold Engineering Development Center, July 1963.

SECTION III
PROCEDURE

3.1 PRE-TEST ALIGNMENT

One of the principal concerns in determining engine thrust vector is a precise definition of system alignment. The initial phase, the alignment of the axial force calibration system centerline with the centerline of the axial force data system, was accomplished by reference measurements in three planes from known points to the centerline of each system. The next phase, alignment of the outer cage, was accomplished by installing an optical alignment rig inside the outer cage and aligning the centerline of the outer cage with the centerline of the axial force data measuring system. With the alignment rig installed, the parallelism and perpendicularity of the load cell ground mounting surfaces were determined. The inner thrust cage was removed from the test cell and mounted on an optical alignment bench where the parallelism and perpendicularity of the load cell mounting surfaces, the engine mounting pads. and the axial data load train mounting surfaces were obtained and the centerline of the inner cage was determined. The inner cage was then installed and aligned with respect to the centerline of the axial force data load train. The engine was aligned with respect to the gimbal ring mounting pads by using an optical alignment rig supplied by Aerojet-General Corporation (AGC). The engine was aligned in the inner thrust cage using a dowel-pin installation on one of the engine mounting pads. After the engine was installed, a final alignment check was made with clinometer measurements on a machined surface on the top of the inner cage. The machined surface was installed parallel to the plane of the engine mounting pads.

Using the above procedure, the centerline of the inner cage was aligned to the centerline of the force system within 0.070 in. and was parallel within 0.047 deg. This would produce a circle in the plane of the throat with a radius of 0.070 in. within which the center of the coordinate system lies for each engine installation. The angle of 0.047 deg is the maximum possible bias error for any engine installation.

3.2 CALIBRATION

An in-place calibration is made on the thrust system prior to each engine test series to determine the constants for corrected side force calculations. These calibrations are performed with propellant lines pressurized and the engine in firing configuration. An in-place calibration consists of applying known loadings to each of the calibrate load

trains in turn and recording the force output at each loading in all of the six data load cells. It is required, for first-order solutions, that all loads be applied so that only one calibrate force is varied at a time. When a calibrate load is applied, the output of the corresponding data load cell is the principal load, and the outputs of the other data load cells are interactions. The calibrate load is applied in an analog fashion (that is, the loading is varied continuously with time) from zero to full load and back to zero. The time taken to apply the calibrate load is approximately two minutes, which allows the response of the system to follow the loading. In determining balance constants, the calibration is reduced at discrete intervals to produce a digital record of reaction versus applied load. Two calibrations are conducted prior to each series to determine the repeatability of the system.

Calibrate loads are applied in both the positive (compression) and negative (tension) directions to allow for the possibility of a slope change on a load cell when going from a negative to a positive applied load. Provisions are made in the data reduction program for the selection of the balance constant based on the sign of the measured load.

3.2.1 Comparison of Calibration

Two complete calibrations are conducted on the six-component thrust stand prior to any engine test series. By comparing these calibration results, a check on the repeatability of the system is obtained. The comparison points are (1) the principal calibration constants, that is, the constants obtained for a data load cell when force is applied to the corresponding calibrate load cell, and (2) the calibration constants obtained from an axial calibrate load application.

Table I presents the principal calibration constants for three groups of two calibrations. The percentage change in each calibration constant is presented in Table II. The changes generally experienced were on the order of from 0.25 to 0.5 percent. (When changes as large as 2 percent were encountered, the problem area was corrected.) The principal slopes for a typical calibration are presented in Fig. 4.

The calibration constants for the multicomponent force system are determined from calibrations conducted under ambient pressure conditions. Since data are obtained at simulated altitude conditions, it is necessary to determine the effect of low pressure on the force system. An axial calibrate loading is performed after a cell pressure of 0.5 psia is obtained. A comparison of the calibration constants obtained during sea-level axial calibrations and the calibration constants obtained at altitude pressures can be made, and Table III presents the results of such a comparison.

3.3 DATA ACCURACY

The accuracy with which the multicomponent force system is capable of determining forces is defined by a combination of several possible errors. The first of these errors, arising from the fact that no physical system is perfectly linear and repeatable, is incurred because the data are linearized by the method of least squares to compute the balance constants. Figure 5 presents a typical deviation from a linearized relationship. Another source of error is the basic accuracy limits of the data acquisition equipment. The combined effect of linearization and data acquisition errors can be determined by using the balance constants obtained from a calibration to reduce the calibration as data. The difference between the input and the calculated value is the combination of linearity and data acquisition errors. Table IV presents the one standard deviation of the errors calculated in this manner. This error is ±0.6 percent of the full range of the load cell for the average standard deviation of all calibrations presented.

Another discrepancy introduced into the system is the capability of the calibrate load cell in determining the true force applied. This error was defined by laboratory calibrations of the load cells against a secondary standard and determined to be ±0.16 percent of full scale.

The error in repeatability of the system from calibration to calibration was found to be 0.5 percent, one standard deviation, while the error in repeatability of the system between sea-level calibration and altitude calibration was on the order of 1.54 percent of full scale for one standard deviation.

The combination of all these errors is given as the accuracy of an individual component of the force system. The combined error is determined by the square root of the sum of the squares of all errors involved. The combined error of the force measured by each load cell is ±1.73 percent, one standard deviation.

The square root of the sum of the squares of the error for both load cells in a plane will give the total error of force measurements in a given plane. For the yaw and pitch planes the total error is ±2.5 percent of the full range of the load cell. An error of 2.5 percent will give a precision of 0.033 deg for the thrust vector angle and 0.0263 in. in the location of the point of intersection of the thrust vector with the engine gimbal plane.

SECTION IV
CALIBRATION EVALUATION

The thrust vector for an operating engine can be determined from the geometry of the system and the measured forces after correction for interaction effects. The equations used for transferring the corrected forces to the engine gimbal plane and converting them to a resultant thrust vector were developed from the considerations of static equilibrium. They are presented in Fig. 6.

The six-component system is designed on the concept that for any load application (L), the force output from any data load cell (R) can be obtained from the following equation:

$$R = C\,L \tag{1}$$

where C is a constant. The force in each of the six load cells can be represented in terms of the applied load by varying the constant. Equation (1) then expands to the form

$$R_i = C_i L \tag{2}$$

where i varies from 1 to 6 and represents the data load cell being observed (Table V). Since there are six calibrate load applicators, Eq. (2) can be expanded to represent the force measured in any load cell under any applied load.

$$R_i = C_{i,j} L_j \tag{3}$$

where j represents the position of load application and varies from 1 to 6 (Table V).

The quantity $C_{i,j}$ is, then, a six-by-six matrix, whereas R_i and L_j are column matrices. The calibration constant matrix ($C_{i,j}$) is determined for both positive and negative applied forces, giving a total of 72 constants, 36 positive and 36 negative.

4.1 LOCATION OF BALANCE ELECTRICAL CENTER

In order to distinguish the actual side forces from interactions, the calibrations described in Section 3.2 were conducted and the calibration constants obtained. The use of the calibration constants in this manner requires linear and repeatable interactions. The method of least squares was used to determine the best linear slope of the data calibration interaction data. The slopes were used in determining the calibration constants ($C_{i,j}$). The method of calculating the calibration constants is presented in Section 4.1.1.

When two load cells are in a common plane, their location with respect to the location of the calibrate load cells can be determined through the use of the electrical center concept. The electrical center of a load cell is the point at which an applied load would be sensed completely by that load cell. Using the interaction slopes (S = dR/dL) and the distance (X) between the point of application of the calibrate loads, an expression for the interaction slope as a function of distance (dS/dX) can be written.

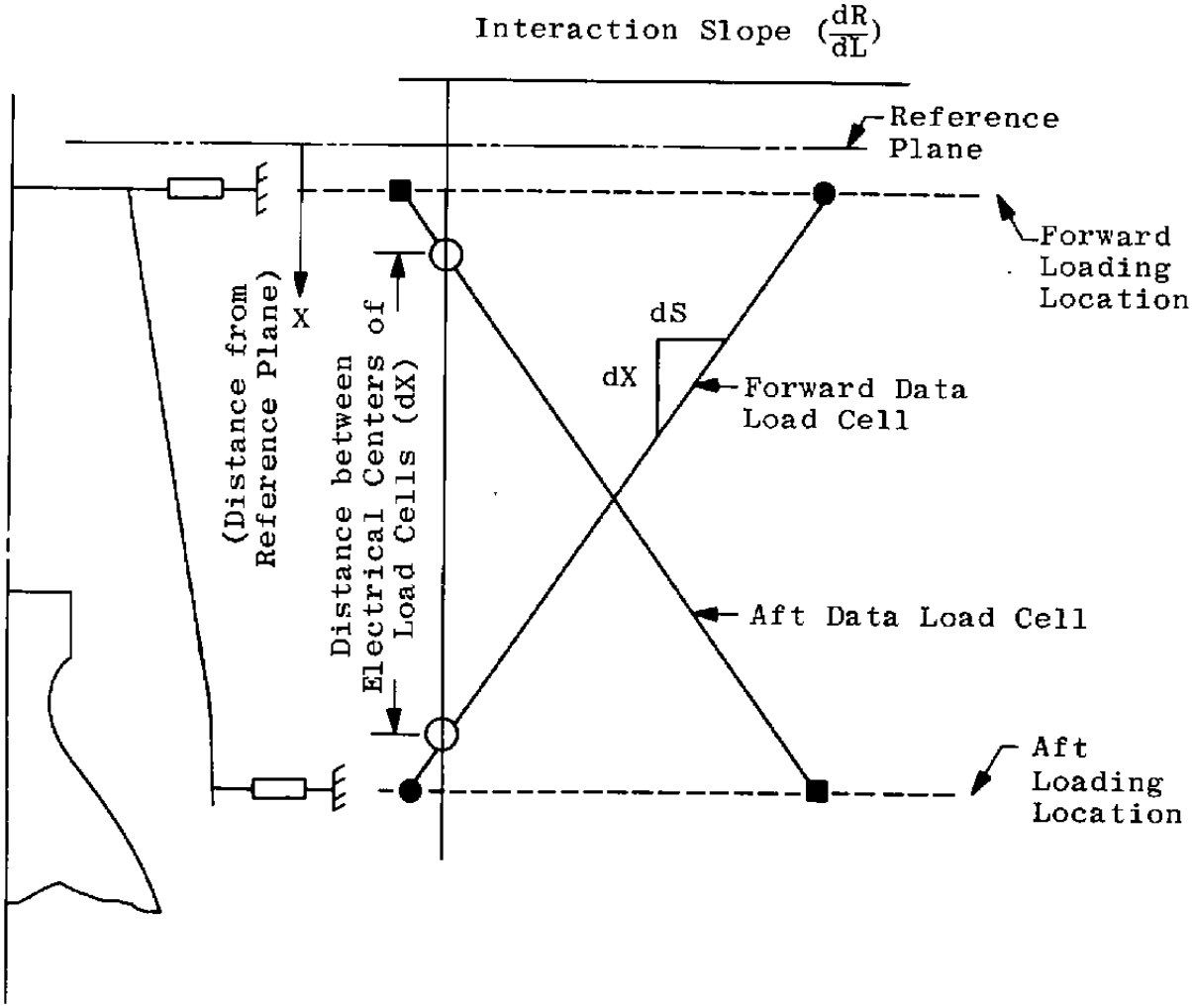

The interaction slope as a function of a distance, using a point slope formula, becomes

$$S_{z,i} = \left(\frac{dS}{dX}\right)_{z,i} X + K_{z,i} \qquad (4)$$

where z and i are defined in Table V, and X is measured from an

arbitrary reference plane. For the subject system the reference plane, chosen so that no negative distance would be encountered, was located 10 in. forward of the upper calibrate load applicator. The electrical center is the point of zero interaction slope for the other data load cell in that plane. The electrical center is also the mathematical location of the force measuring gage.

Once the electrical center is determined for each load cell in a plane, two useful facts can be determined: (1) the distance between the electrical center of the load cells (ΔX), and (2) the distance from the reference plane to a point halfway between the two electrical centers (X). The electrical center is determined for both positive and negative load applications in both the pitch and yaw planes.

4.1.1 Calculation of Calibration Constants

4.1.1.1 Pitch and Yaw Gages

The force in any load cell can be calculated for any load application if the interaction slope, the location of the force vector, and the applied force are known. An equation of the following form is required:

$$R_i = S_{z,i} L_j \tag{5}$$

From the electrical center investigation, the slope (S) was determined as a function of load position, Eq. (4),

$$S_{z,i} = \left(\frac{dS}{dX}\right)_{z,i} X + K_{z,i}$$

where X is the location of the force. Substitution of Eq. (4) into Eq. (5) then yields

$$R_i = \left[\left(\frac{dS}{dX}\right)_{z,i} X + K_{z,i}\right] L_j \tag{6}$$

The equations of the calibration constants for the pitch load cells are developed for the purpose of demonstration. The location of the pitch force vector with respect to the reference plane can be determined from the moment equations:

$$M = L_t X \tag{7}$$

L_t may be represented as the sum of L_{P_1} and L_{P_2}.

$$L_t = L_{P_1} + L_{P_2} \tag{8}$$

The distance between the force measuring cells L_{P_1} and L_{P_2} is defined as ΔX_P. The moment generated about the reference point can then be written as

$$M = L_{P_1} (X_{ref.}) + L_{P_2} (X_{ref.} + \Delta X_P) \tag{9}$$

Having established that

$$X_{ref.} = X_P - \frac{\Delta X_P}{2} \tag{10}$$

substitution yields

$$M = L_{P_1} \left(X_P - \frac{\Delta X_P}{2}\right) + L_{P_2} \left(X_P + \frac{\Delta X_P}{2}\right) \tag{11}$$

Combining

$$M = (L_{P_1} - L_{P_2}) X_P - (L_{P_1} - L_{P_2}) \frac{\Delta X_P}{2} \tag{12}$$

The location of the force vector is defined from the moment equation as follows:

$$X = \frac{M}{L_t}$$

Therefore

$$X_{PF} = - \frac{L_{P_1} - L_{P_2}}{L_{P_1} + L_{P_2}} \left(\frac{\Delta X_P}{2}\right) + X_P \tag{13}$$

The expression for the location of the force vector (Eq. (13)) can now be substituted for X in Eq. (6).

$$R_i = \left[\left(\frac{dS}{dX}\right)_{p,i} \left(- \frac{\Delta X_P (L_{P_1} - L_{P_2})}{2(L_{P_1} + L_{P_2})} + X_P\right) + K_{p,i}\right] L_t \tag{14}$$

Replacing L_t by $L_{P_1} + L_{P_2}$, Eq. (14) can be rewritten as

$$R_i = \left(\frac{dS}{dX}\right)_{p,i} \left(\frac{\Delta X_P}{2}\right)\left[-(L_{P_1} - L_{P_2})\right] + \left(\frac{dS}{dX}\right)_{p,i} (X_P)(L_{P_1} + L_{P_2}) + K_{p,i} (L_{P_1} + L_{P_2}) \tag{15}$$

Separating L_{P_1} and L_{P_2} yields

$$R_i = \left[- \left(\frac{dS}{dX}\right)_{p,i} \left(\frac{\Delta X_P}{2}\right) + \left(\frac{dS}{dX}\right)_{p,i} X_P + K_{p,i}\right] L_{P_1} + \left[\left(\frac{dS}{dX}\right)_{p,i} \frac{\Delta X_P}{2} + \left(\frac{dS}{dX}\right)_{p,i} X_P + K_{p,i}\right] L_{P_2} \tag{16}$$

R can also be represented in the form

$$R_i = C_{i,1} L_{P_1} + C_{i,5} L_{P_2} \tag{17}$$

where $C_{i,1}$ represents the calibration constants for any gage with a forward pitch calibrate load, and $C_{i,5}$ defines the calibration constants for any gage with an aft pitch calibrate load.

Setting Eq. (16) equal to Eq. (17), an expression for $C_{i,1}$ and $C_{i,5}$ can be determined:

$$C_{i,1} = -\left(\frac{dS}{dX}\right)_{p,i} \frac{\Delta X_P}{2} + \left(\frac{dS}{dX}\right)_{p,i} X_P + K_{p,i}$$

$$C_{i,5} = \left(\frac{dS}{dX}\right)_{p,i} \frac{\Delta X_P}{2} + \left(\frac{dS}{dX}\right)_{p,i} X_P + K_{p,i} \tag{18}$$

A similar development for the yaw plane yields similar results in X_Y:

$$C_{i,2} = -\left(\frac{dS}{dX}\right)_{y,i} \frac{\Delta X_Y}{2} + \left(\frac{dS}{dX}\right)_{y,i} X_Y + K_{y,i}$$

$$C_{i,6} = \left(\frac{dS}{dX}\right)_{y,i} \frac{\Delta X_Y}{2} + \left(\frac{dS}{dX}\right)_{y,i} X_Y + K_{y,i} \tag{19}$$

4.1.1.2 Axial and Roll Calibration Constants

For calibration loads applied in either the axial or roll direction, the calibration constants are determined directly from the observed force in each load cell. The calibration constants are simply the slopes of the calibration loads versus data load cell outputs. An expression for these calibration constants is given below:

$$C_{i,3} = S_{3,i} \quad \text{Axial}$$

$$C_{i,4} = S_{4,i} \quad \text{Roll} \tag{20}$$

4.2 DETERMINATION OF BALANCE CONSTANTS

Once the calibration constants $C_{i,j}$ are determined, they can be represented in matrix form:

$$\begin{bmatrix} R_1 \\ R_2 \\ R_3 \\ R_4 \\ R_5 \\ R_6 \end{bmatrix} = \begin{bmatrix} C_{1,1} & C_{1,2} & C_{1,3} & C_{1,4} & C_{1,5} & C_{1,6} \\ C_{2,1} & C_{2,2} & C_{2,3} & C_{2,4} & C_{2,5} & C_{2,6} \\ C_{3,1} & C_{3,2} & C_{3,3} & C_{3,4} & C_{3,5} & C_{3,6} \\ C_{4,1} & C_{4,2} & C_{4,3} & C_{4,4} & C_{4,5} & C_{4,6} \\ C_{5,1} & C_{5,2} & C_{5,3} & C_{5,4} & C_{5,5} & C_{5,6} \\ C_{6,1} & C_{6,2} & C_{6,3} & C_{6,4} & C_{6,5} & C_{6,6} \end{bmatrix} \begin{bmatrix} L_1 \\ L_2 \\ L_3 \\ L_4 \\ L_5 \\ L_6 \end{bmatrix}$$

The above equation is the matrix representation of Eq. (3),

$$R_i = C_{i,j} L_j$$

To determine the true applied force (L_i) from the load cell measurements, an equation of the following form is necessary:

$$L_j = k_{j,i} R_i \tag{21}$$

where $k_{j,i}$ are the balance constants. Comparing Eqs. (3) and (15), $k_{j,i}$ is seen to be the inversion of the matrix $C_{i,j}$.

Therefore, to obtain the applied load (L_j) from measured forces, the calibration constants are simply inverted and multiplied by the forces measured.

$$\begin{bmatrix} L_1 \\ L_2 \\ L_3 \\ L_4 \\ L_5 \\ L_6 \end{bmatrix} = \begin{bmatrix} k_{1,1} & k_{1,2} & k_{1,3} & k_{1,4} & k_{1,5} & k_{1,6} \\ k_{2,1} & k_{2,2} & k_{2,3} & k_{2,4} & k_{2,5} & k_{2,6} \\ k_{3,1} & k_{3,2} & k_{3,3} & k_{3,4} & k_{3,5} & k_{3,6} \\ k_{4,1} & k_{4,2} & k_{4,3} & k_{4,4} & k_{4,5} & k_{4,6} \\ k_{5,1} & k_{5,2} & k_{5,3} & k_{5,4} & k_{5,5} & k_{5,6} \\ k_{6,1} & k_{6,2} & k_{6,3} & k_{6,4} & k_{6,5} & k_{6,6} \end{bmatrix} \begin{bmatrix} R_1 \\ R_2 \\ R_3 \\ R_4 \\ R_5' \\ R_6 \end{bmatrix} \tag{22}$$

During an engine firing, forces are measured at each of the six data force measuring load cells. The actual forces are determined from these measured forces by correcting for the interaction effects. This is done by applying the balance constants developed in this section to the measured forces.

SECTION V
RESULTS AND DISCUSSION

5.0 THRUST VECTOR DETERMINATION

The objective of the six-component force balance was to determine the thrust vector generated by the AJ10-137 engine and to define the excursion of this vector with time. The calibration of the force balance was conducted, and the balance constants were applied to the measured forces in the manner presented in Section IV to obtain the actual forces produced by the engine. Once these forces were known, the principles of static equilibrium were applied, and the six forces resolved into a thrust vector at the engine gimbal plane. This thrust vector is

presented in the form of the angle from vertical in the pitch and yaw planes* and the point of intersection of the thrust vector with the gimbal plane, represented as distances (ξ, η) measured from the balance centerline. The thrust vector excursion for two different chambers (Table VI) is presented in this report along with thrust vector measurements during gimbal operations from one test firing.

5.1 THRUST VECTOR MEASUREMENTS DURING NONGIMBALING OPERATION

The two chambers investigated displayed different thrust vector excursion patterns. Since the basic engine configuration was the same, the excursion patterns are attributed to differences in chamber throat erosion. The initial angular offset from the thrust cage centerline was determined to be 1.1 deg from vertical in the pitch plane and 0.22 deg in the yaw plane (Fig. 7) for chamber 1. This initial angle is a function of the alignment of the engine in the thrust cage and of the deflection characteristics of the engine mounting system under firing loads. The thrust vector angular excursion (Fig. 7) for chamber 1 indicated significant nonsymmetrical chamber throat erosion during this chamber life cycle. The thrust vector angle excursion in the pitch plane (0.57 deg) was greater than the excursion in the yaw plane (0.22 deg). The excursions did follow a definite pattern for similar firings. For each 20-sec firing the angle decayed from the initial value. For the 160- and 60-sec firings, the angular decay was observed for a period of 50 sec, after which the angle increased. The angle in the yaw plane exhibited a similar pattern, but of lower magnitude. Although the angle decayed from the initial value, the initial value for each successive firing was larger than the previous value. The incremental angular change between the end of one firing and the beginning of the next is attributed to throat area changes caused by expansion and contraction of the throat due to residual heat in the ablative material. The excursion of the intersection point of the thrust vector and the engine gimbal plane is presented in Fig. 8. The excursion of the intersection point was insignificant for the short-duration firings (up to 20 sec). For the 160-sec firing, the excursion was 0.18 in. in the yaw plane (η) and 0.195 in. in the pitch plane (ξ) and occurred in a random pattern.

Chamber 1 was tested under two different conditions. The first two test series (G and H) were conducted with stiff links used in place of the

---

*The pitch and yaw planes used in this report are rotated 45 deg from the engine coordinate system.

gimbal actuators, whereas test series J and K were conducted using gimbal actuators. The angular difference measured after changing to gimbal actuators was 1.25 deg in the pitch plane and 0.53 deg in the yaw plane with a position change of 0.07 in. in the pitch plane and 0.14 in. in the yaw plane. The capability of realigning the force balance is ±0.047 deg with respect to vertical and ±0.07 in. with respect to the point of intersection of the gimbal plane and the force balance centerline. The difference between the thrust vector angle measured after the installation change and the force balance angular alignment capability was 1.203 deg in the pitch plane and 0.48 deg in the yaw plane. The measured thrust vector position (0.07 in.) was within alignment capability of the force balance in the pitch plane (ξ) and exceeded the alignment capability by 0.07 in. in the yaw plane (η). These differences represent the minimum changes which can be attributed to differences in deflection characteristics of the stiff links and the gimbal actuators and of the capability of AGC to realign the engine centerline with the force balance centerline.

The thrust vector excursion for chamber 2 is presented in Figs. 9 and 10. The initial thrust vector was 0.36 deg in the pitch plane and -0.62 deg in the yaw plane. The excursion of the angle in the pitch and yaw planes displayed similar patterns with a total angular growth of 0.44 deg in pitch and 0.30 deg in yaw. The point of intersection is presented in Fig. 11 as a function of cumulative time. The total excursion of the thrust vector position was 0.15 in. in the pitch plane and 0.30 in. in the yaw plane. The tests conducted on chamber 2 were made using gimbal actuators.

The angular excursion patterns for chamber 1 and chamber 2 displayed similar patterns in the pitch plane. The angular patterns in the yaw plane were different, however. Although the total cumulative time on chamber 2 was greater (600 sec on chamber 2, 496 sec on chamber 1) than on chamber 1, the thrust vector angular excursion was less. The excursion of the thrust vector position for the two chambers showed little similarity.

Thrust vector excursion is believed to be primarily and directly relatable to thermal and ablative effects on the combustion chamber. Figures 12a, b, and c show typical pre- and post-fire conditions of an AJ10-137 combustion chamber.

5.2 THRUST VECTOR MEASUREMENT DURING GIMBALING OPERATION

The J-3 six-component force balance was designed to determine thrust vector during nongimbaling (steady-state) operation of the Apollo S/M engine. In order to evaluate the force balance, however, the thrust vector was determined during gimbaling operations for one engine firing and the results are presented in Fig. 13. The gimbal program for this particular firing was a low-frequency (0.5 cps) ramp and a step function in the yaw plane only.

During the gimbaling operation investigated, the thrust vector determined by the force balance followed the gimbal angle indication received from a position indicator on the yaw gimbal actuator. The magnitude of the angle measured by the force balance compares very closely with the position indicator with a maximum difference of 0.24 deg and general agreement within 0.08 deg. The response of the force balance measurements was at least equal to the response of the position indicator.

The thrust vector position determined during gimbaling is the true vector position, within the accuracies stated in Section III. The force balance can be used to determine a relationship between the command signal and the gimbal actuator position indication. The gimbal rate which the force balance can follow is limited by the low natural frequency of the inner thrust cage assembly (from 5 to 10 cps). Therefore, a comparison of these parameters could be made on low-frequency gimbal operations only.

The thrust vector determined by the force balance and shown in Fig. 13 was corrected for zero position at the beginning of the firing. The vector did not return to zero at the end of the firing, indicating thrust vector excursion resulting from thermal and ablative effects on the engine throat.

SECTION VI
SUMMARY OF RESULTS

A multicomponent force balance was developed to measure the thrust vector position and excursion during tests of the Apollo S/M engine which were conducted at AEDC. The results are summarized below:

1. The thrust vector angle was determined for two ablative thrust chambers. The initial values, measured from vertical, were 1.1 deg in pitch and 0.22 deg in yaw for chamber 1 and 0.36 deg in pitch and -0.62 deg in yaw for chamber 2.

2. The thrust vector angle excursion was determined for two chambers. The total angular excursion in the pitch plane was 0.57 deg and 0.44 deg for chambers 1 and 2, respectively. The angular excursion in the yaw plane was 0.22 deg and 0.30 deg for chambers 1 and 2.

3. The excursion of the thrust vector position was also determined. For chamber 1 the position excursion was 0.195 in. in the pitch plane (ξ) and 0.18 in. in the yaw plane (η). For chamber 2 the position excursion was 0.15 in. in the pitch plane and 0.30 in. in the yaw plane.

4. Thrust vector measurements were made during gimbaling operation of the Apollo engine. The thrust vector measurements agreed within 0.08 deg with the position indicator on the gimbal actuator.

5. The precision of thrust vector data was determined to be ±0.033 deg from vertical on the angle and ±0.0263 in. for location of the intersection of the thrust vector with the engine gimbal plane. The alignment accuracies of the force balance are ±0.047 deg from vertical and ±0.07 in. for determination of the coordinate system centerline.

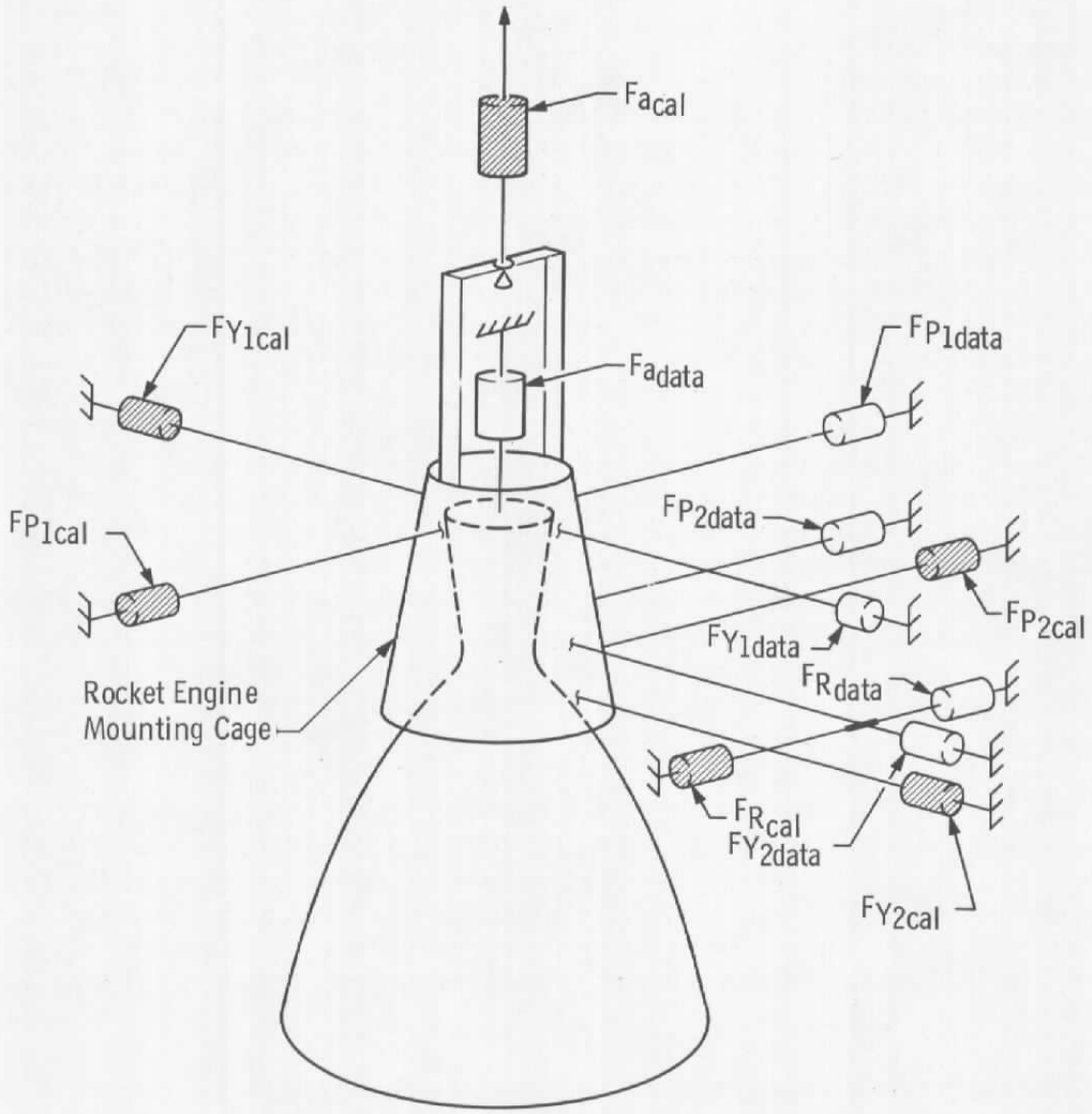

a. Schematic of Six-Component Force System

Fig. 1 Six-Component Force System

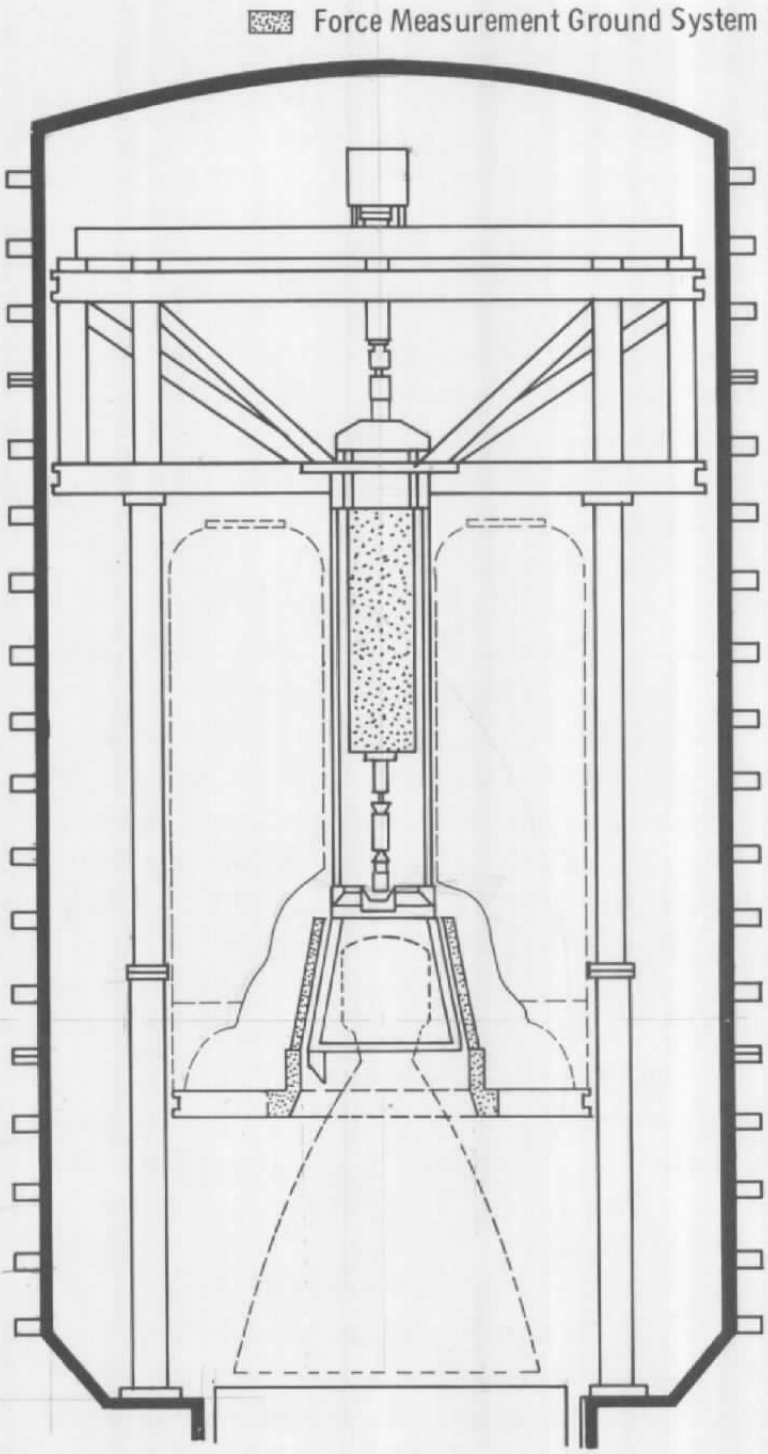

b. Schematic of J-3 Propulsion Engine Test Cell

Fig. 1 Continued

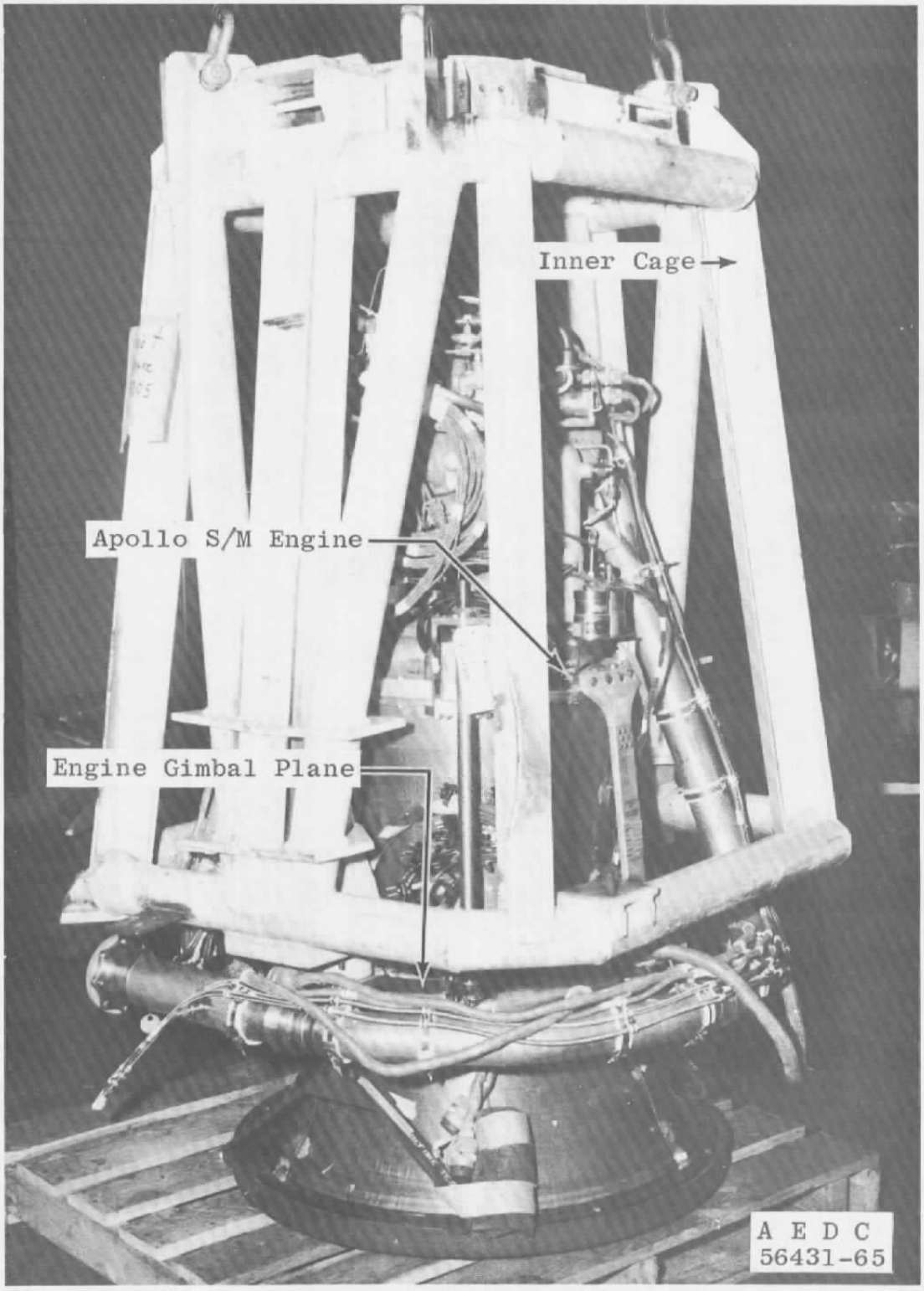

c. Apollo S/M Engine Mounted in Inner Cage

Fig. 1 Concluded

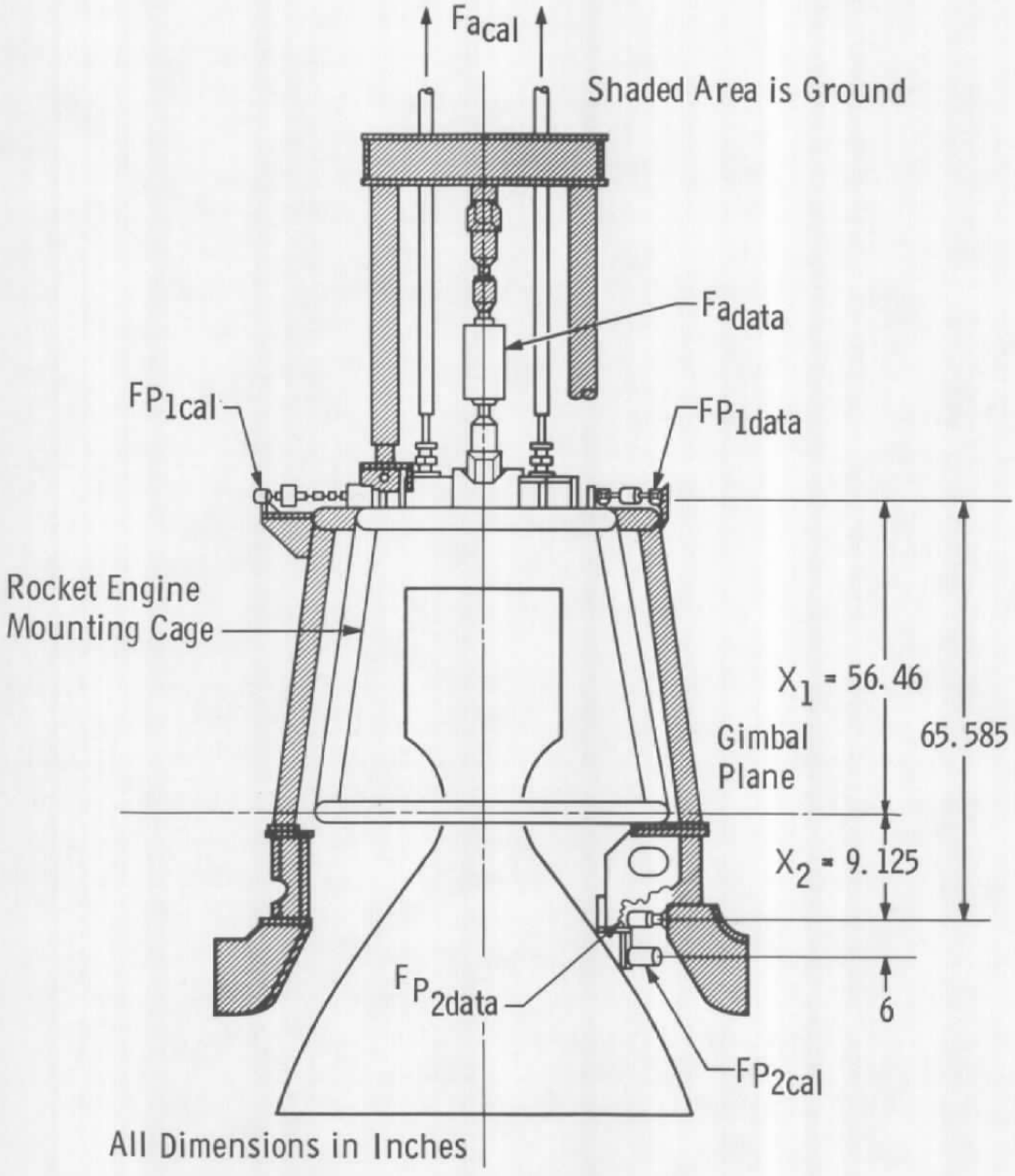

a. Pitch Plane

Fig. 2 Arrangement of Load Cells

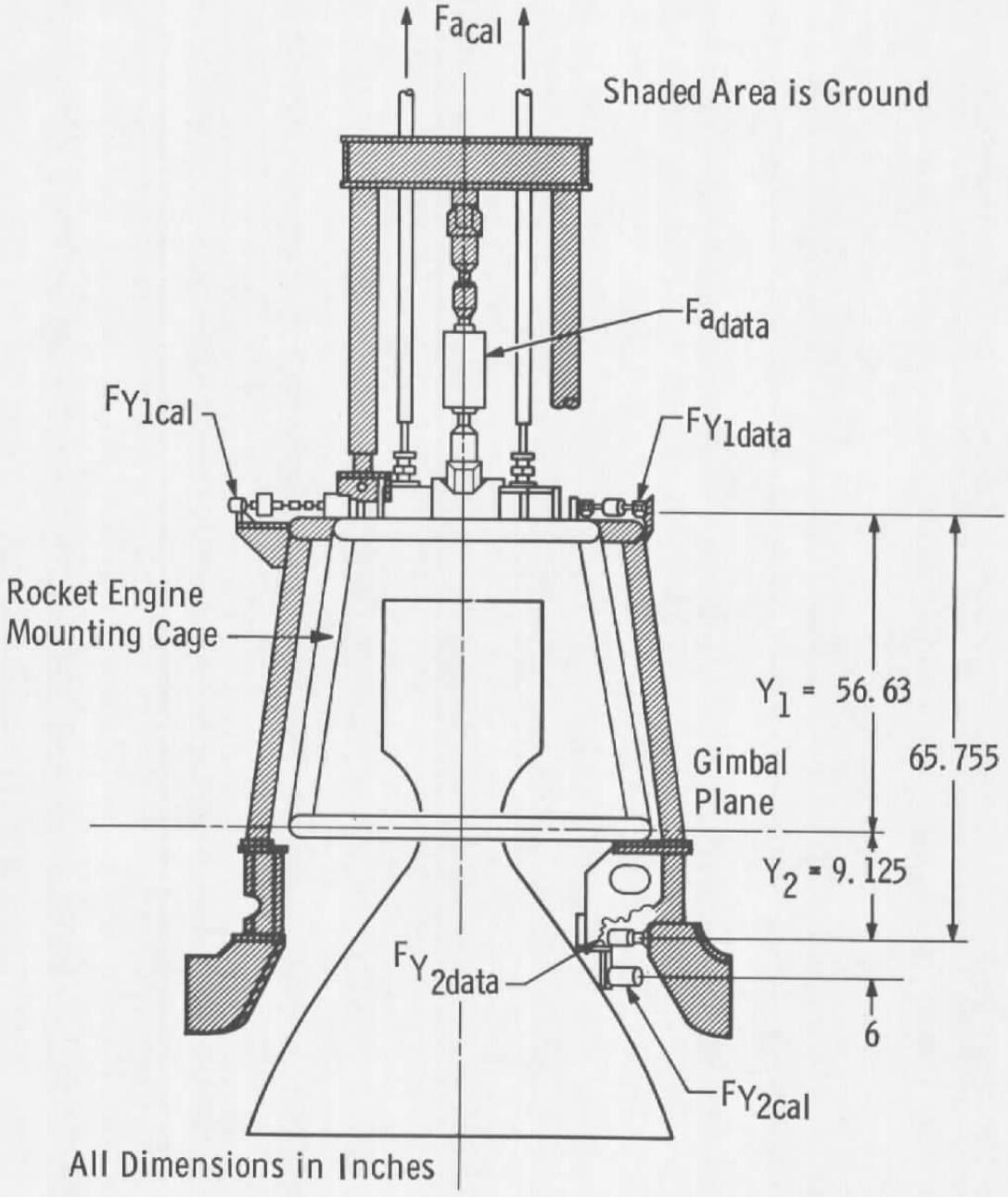

b. Yaw Plane

Fig. 2 Concluded

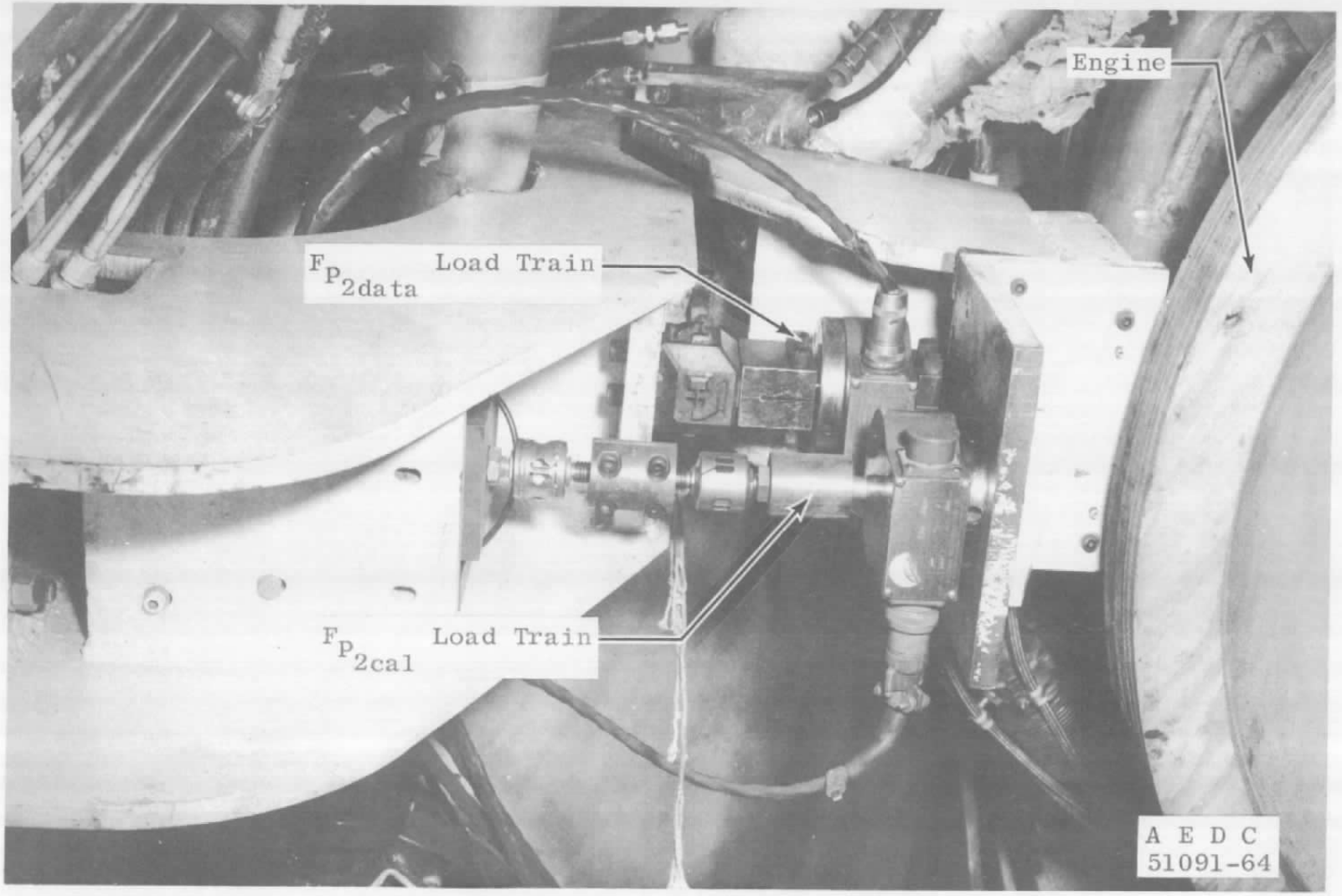

a. Installation of F_{P_2} Calibrate and Data Load Cells

Fig. 3 Installation of Six-Component Force System

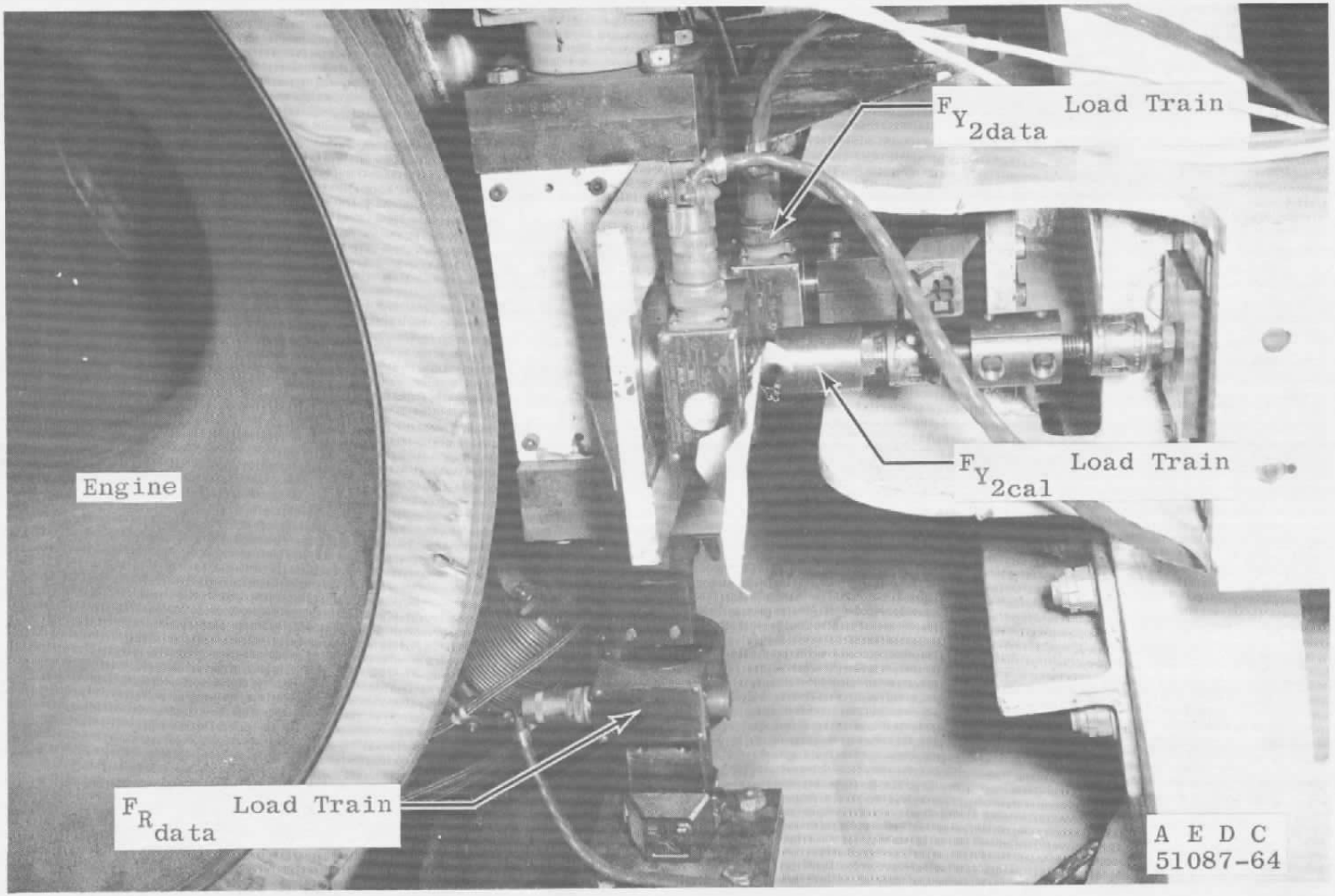

b. Installation of F_{Y_2} Calibrate and Data Load Cells

Fig. 3 Continued

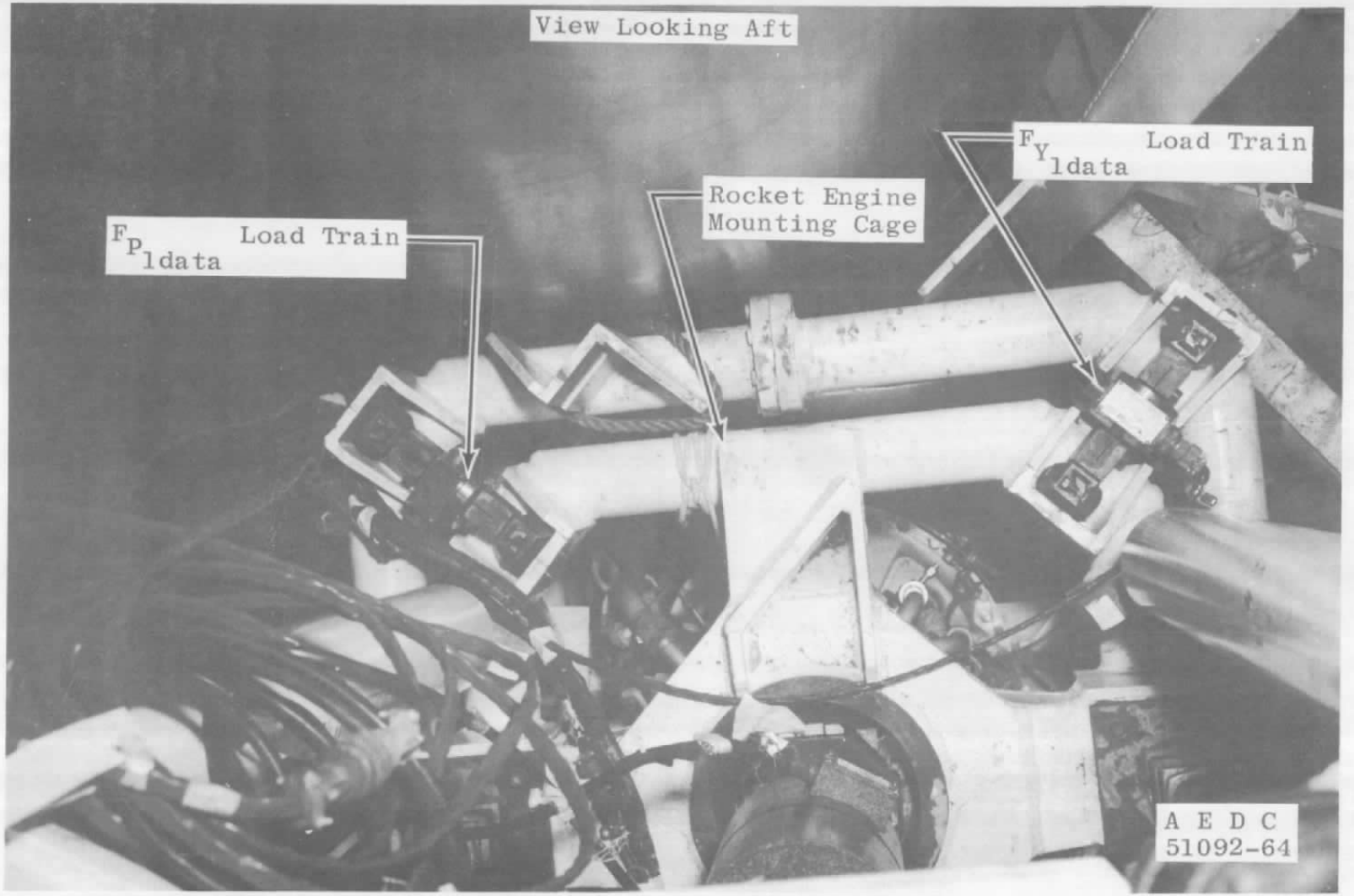

c. Installation of F_{P_1} and F_{Y_1} Data Load Cells

Fig. 3 Concluded

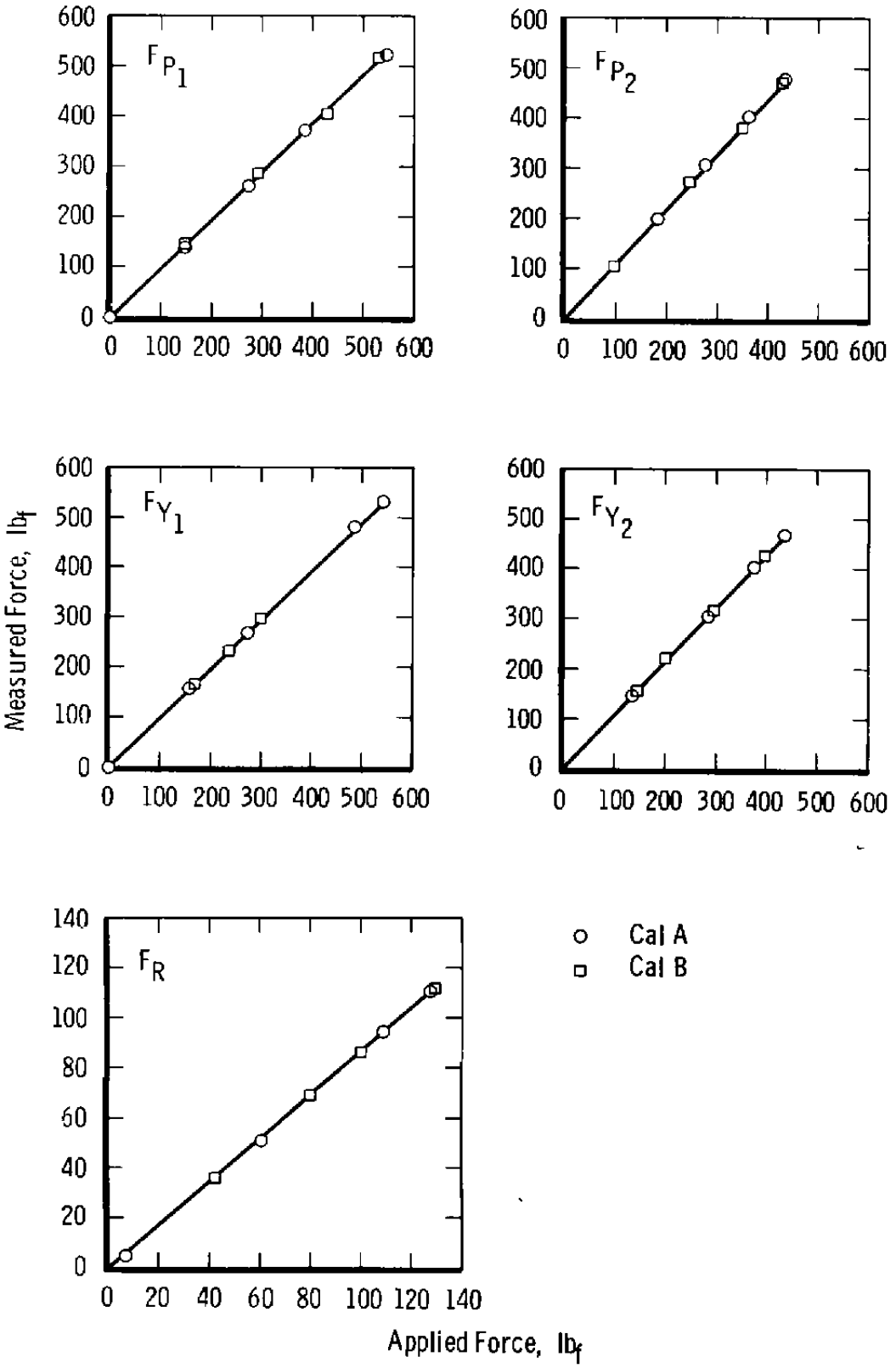

Fig. 4 Comparison of Principal Slopes for a Typical Calibration

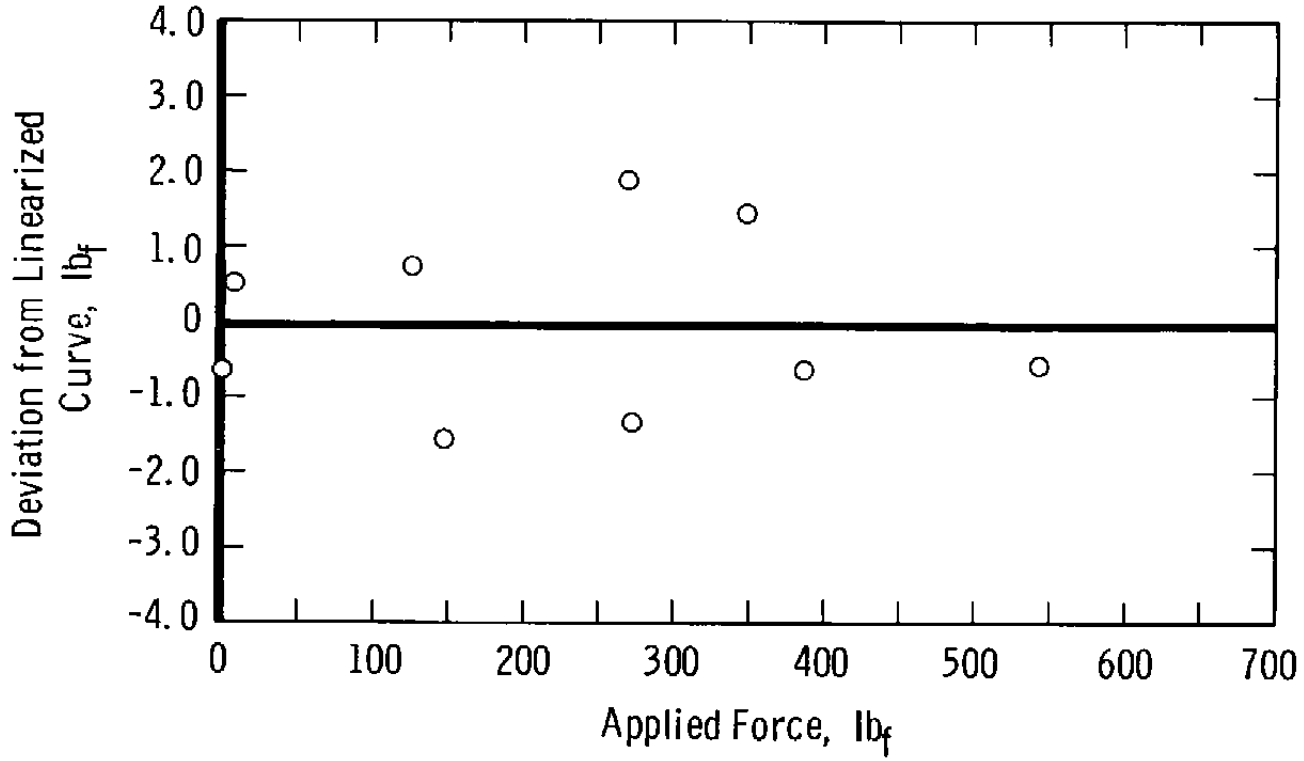

Fig. 5 Deviation of Typical Interaction Force from Linearized Curve

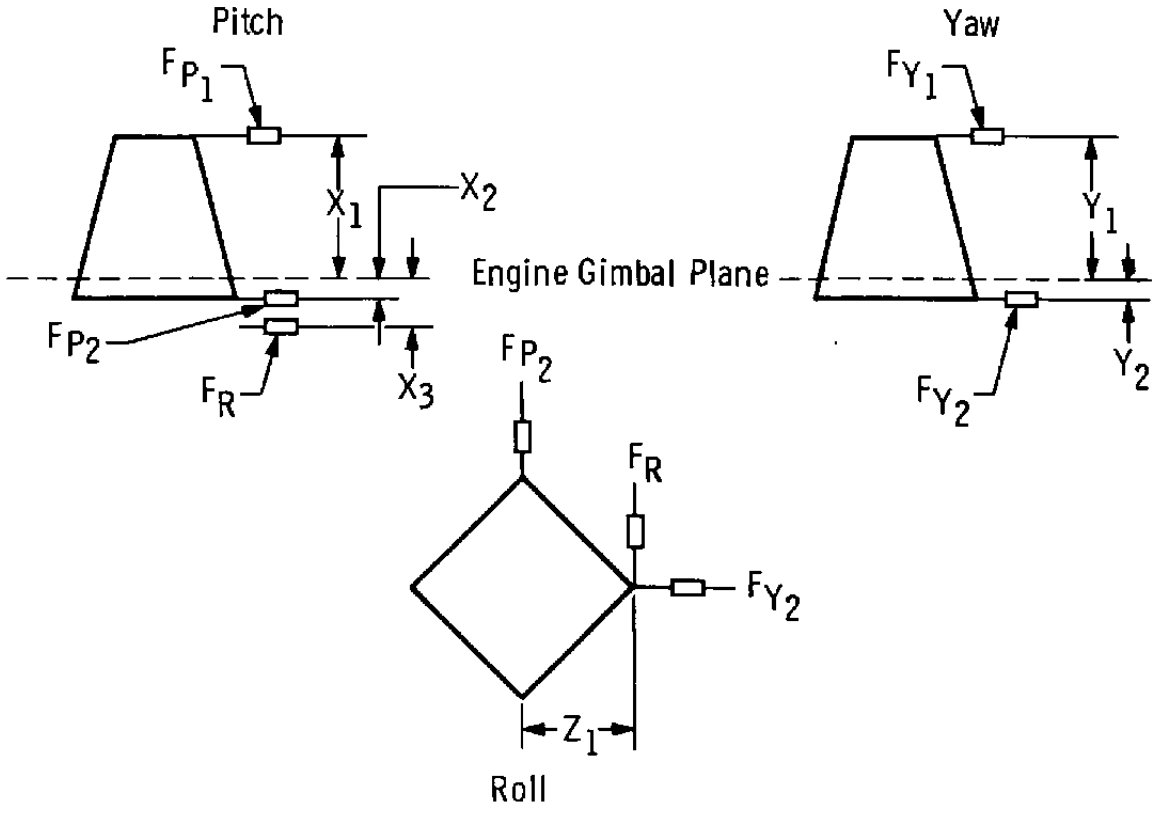

Parameter	Equation
F_a	F_a
F_{P_t}	$F_{P_1} + F_{P_2} + F_R$
F_{Y_t}	$F_{Y_1} + F_{Y_2}$
M_p	$F_{P_1}(X_1) - F_{P_2}(X_2) - F_R(X_3)$
M_y	$F_{Y_1}(Y_1) - F_{Y_2}(Y_2)$
M_r	$F_R(Z_1)$
θ	$\tan^{-1}(F_{P_t}/F_a)$
ϕ	$\tan^{-1}(F_{Y_t}/F_a)$

Fig. 6 Equations for Determining Thrust Vector from Six-Component Force Measurements

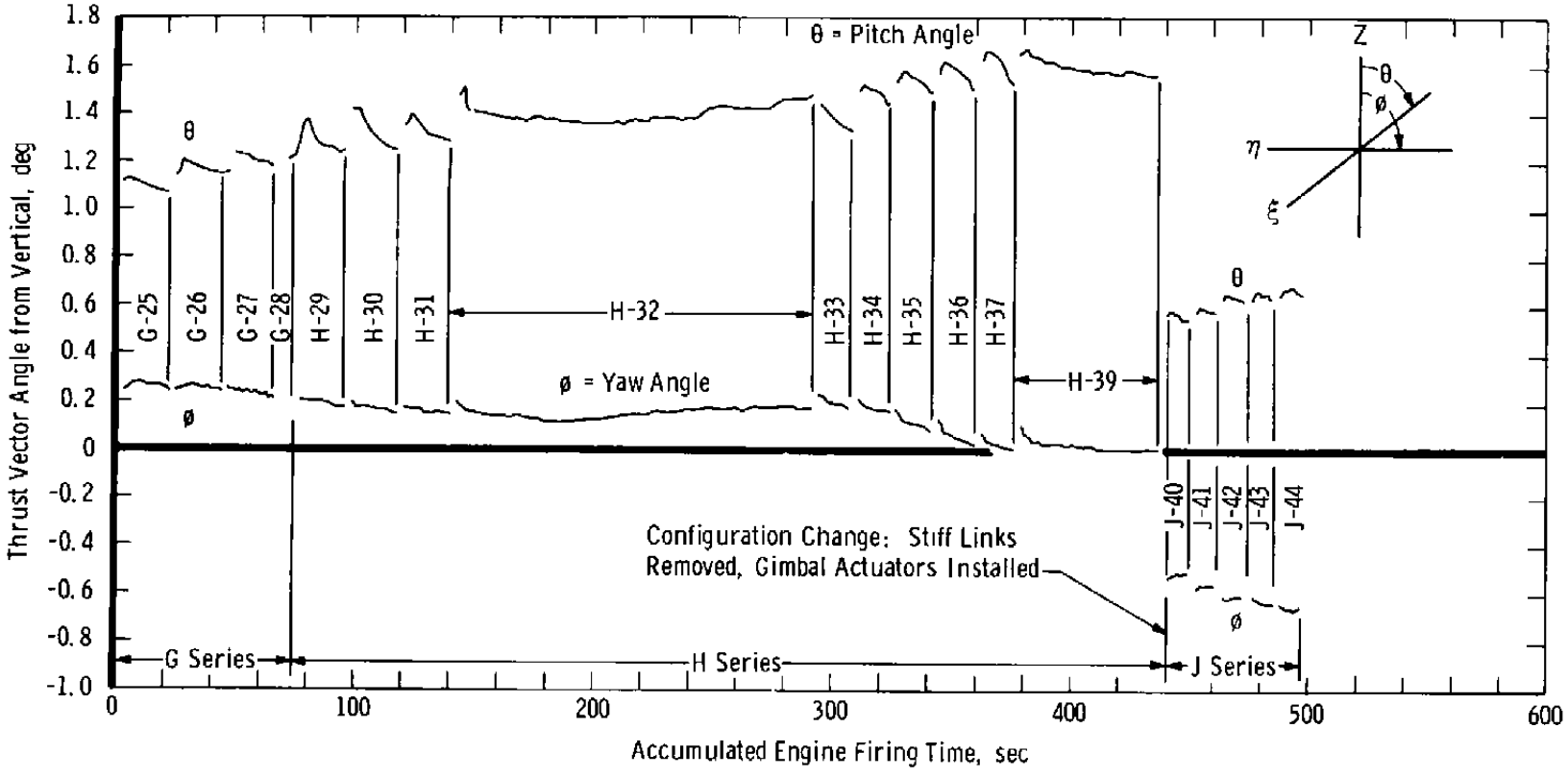

Fig. 7 Thrust Vector Excursion for Chamber 1

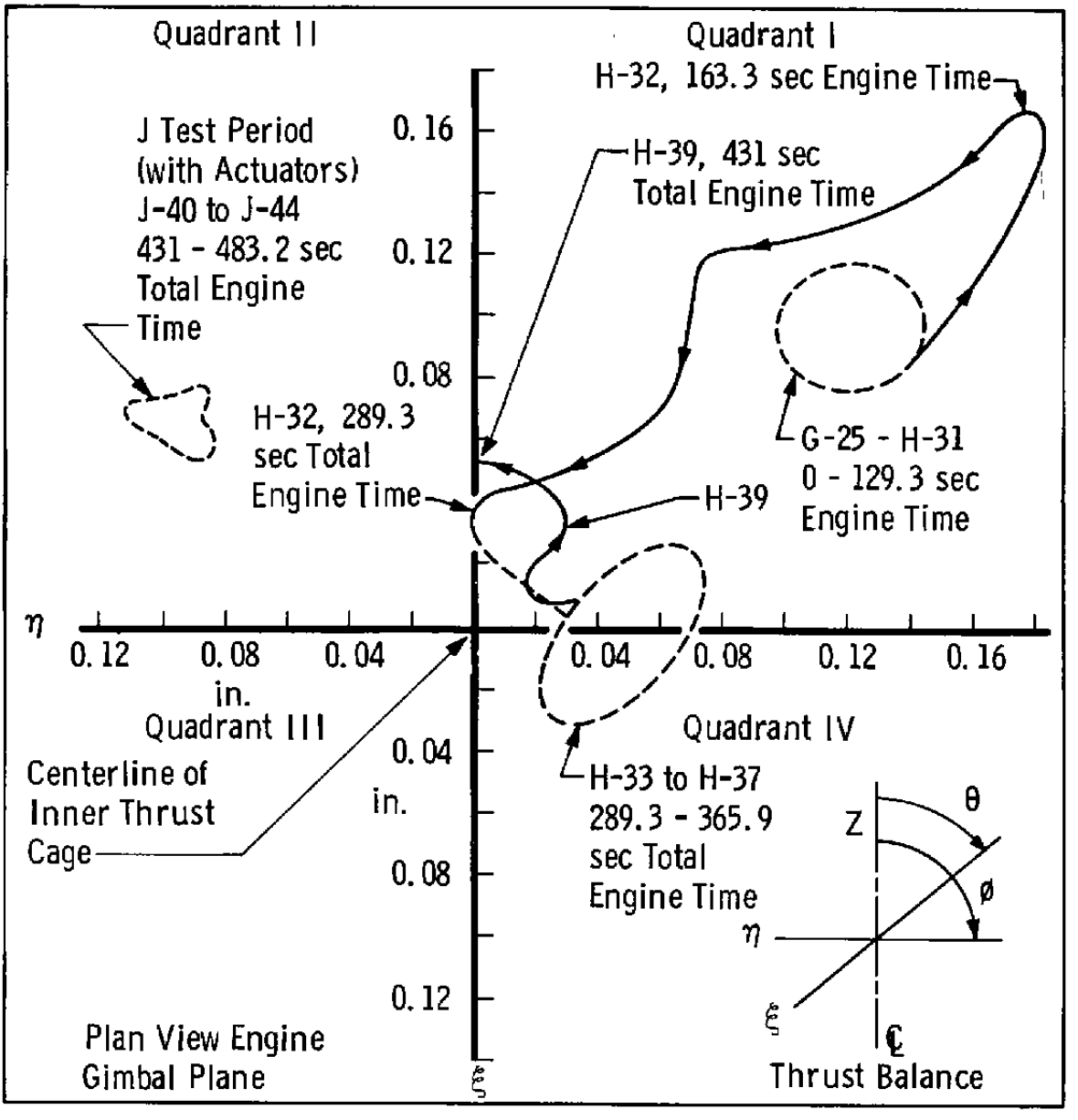

Fig. 8 Effect of Ablation on Thrust Vector Intercept Location for Chamber 1

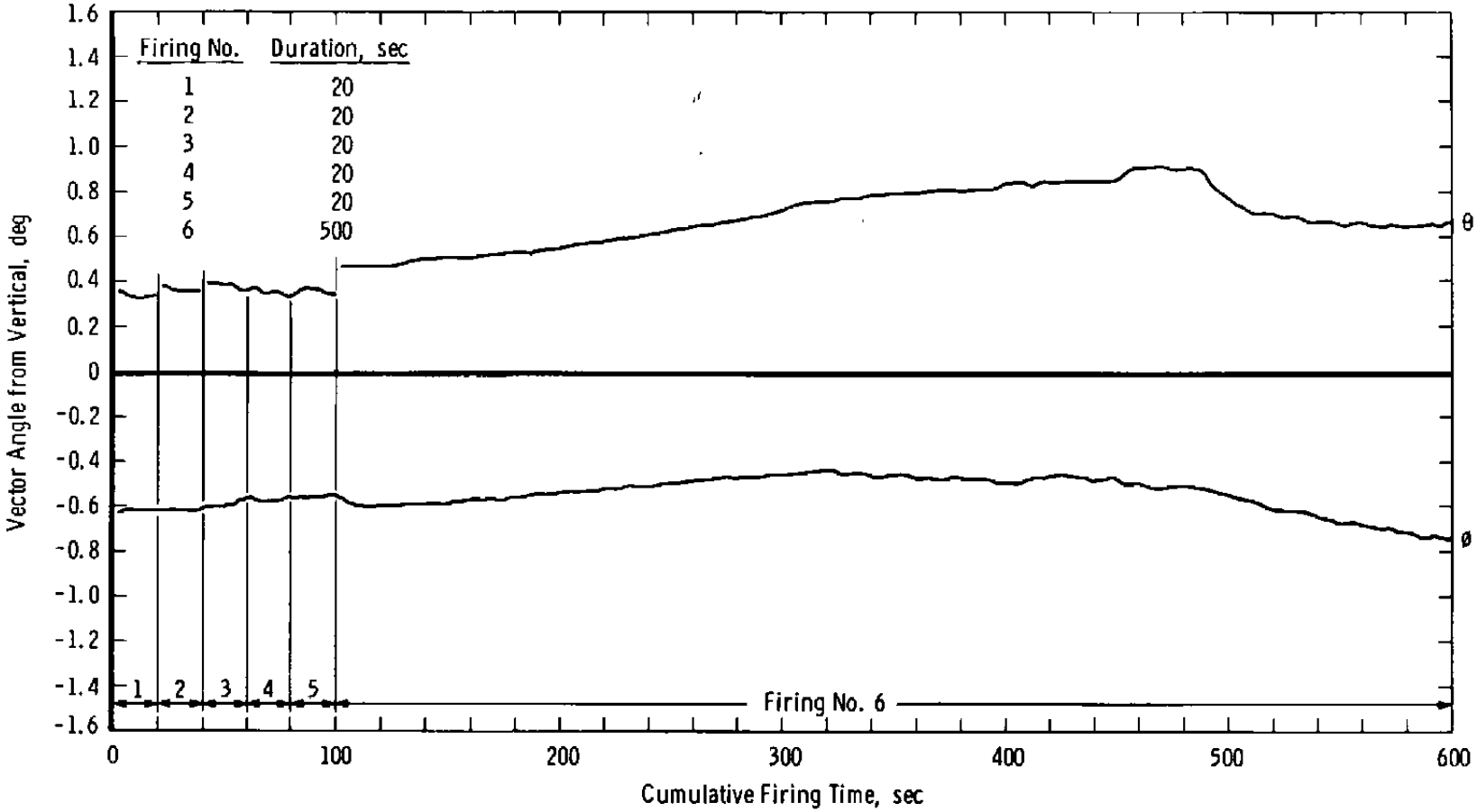

Fig. 9 Thrust Vector Excursion for Chamber 2

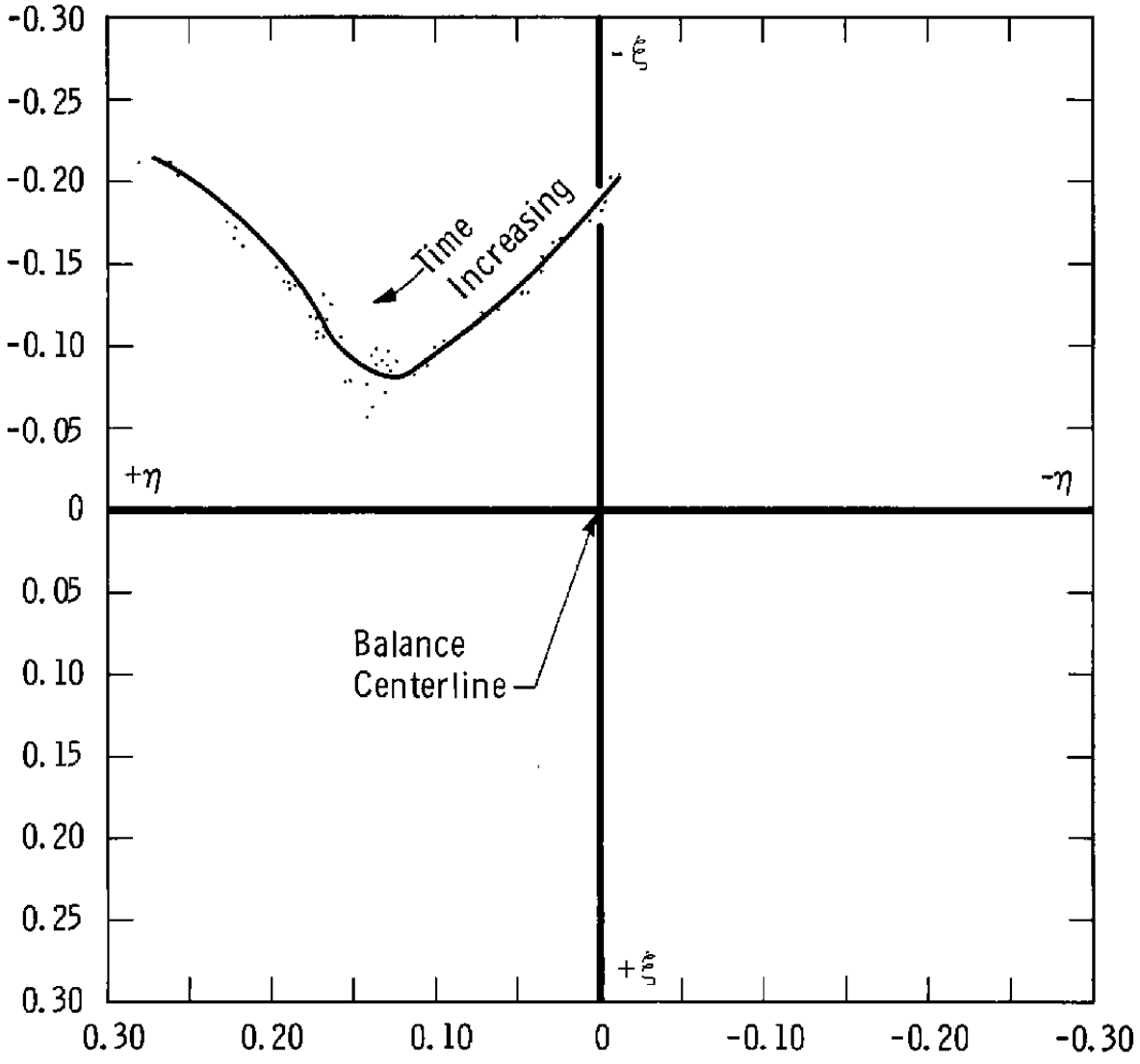

Fig. 10 Effect of Ablation on Thrust Vector Intercept Location for Chamber 2

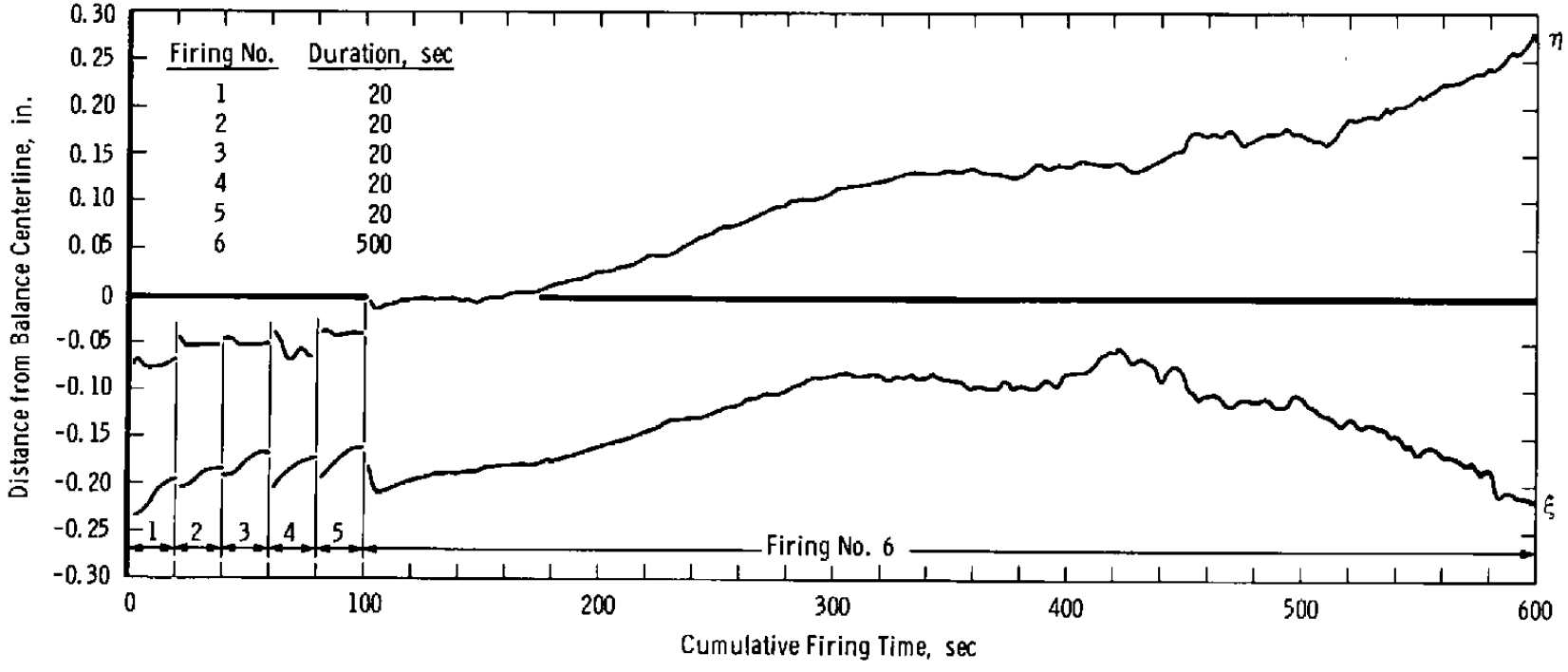

Fig. 11 Time History of Thrust Vector Intersection with Engine Gimbal Plane for Chamber 2

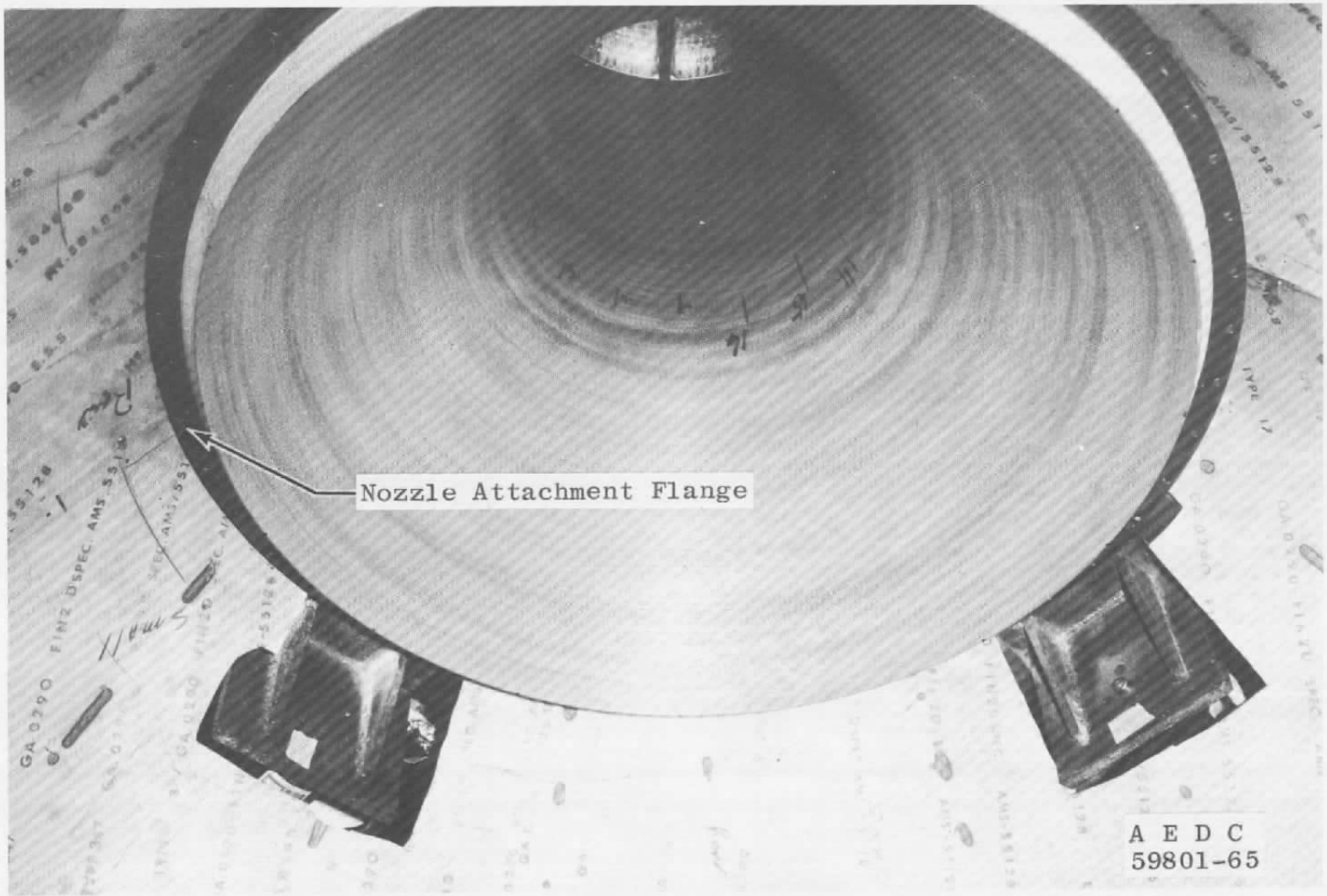

a. Pre-Test Looking Forward

Fig. 12 Pre- and Post-Test Photographs of Typical AJ10-137 Combustion Chamber

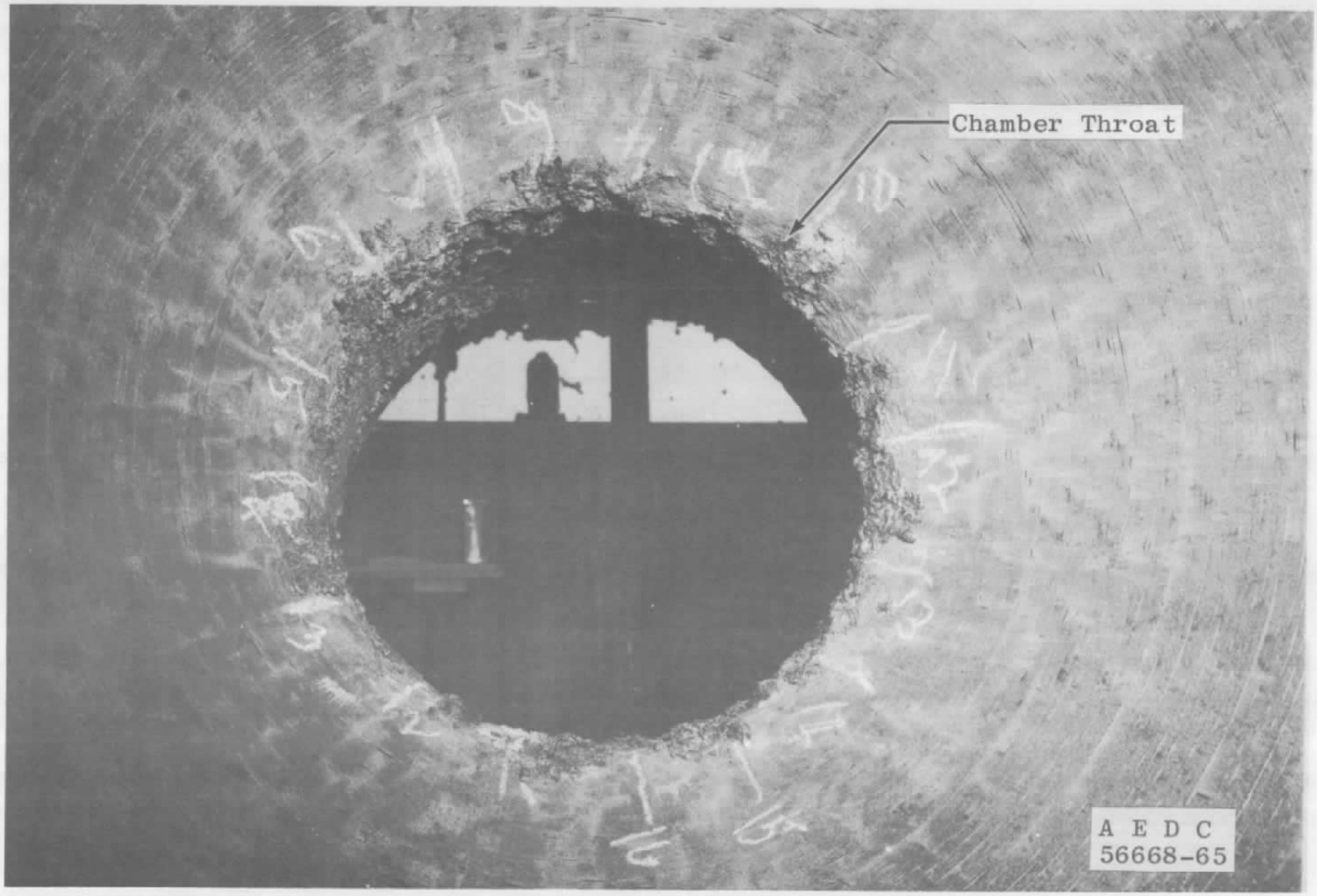

b. Post-Test Looking Forward

Fig. 12 Continued

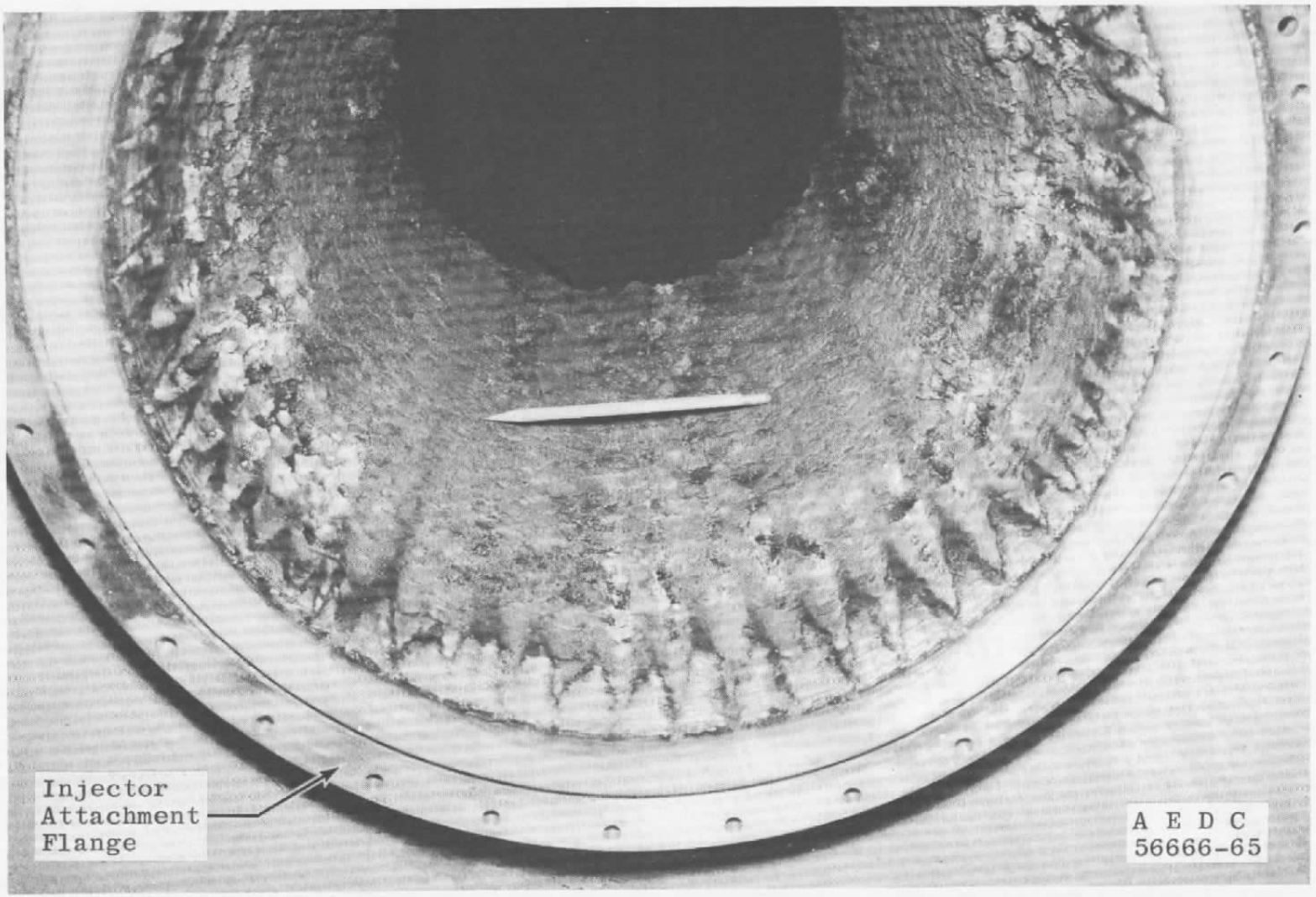

c. Post-Test Looking Aft

Fig. 12 Concluded

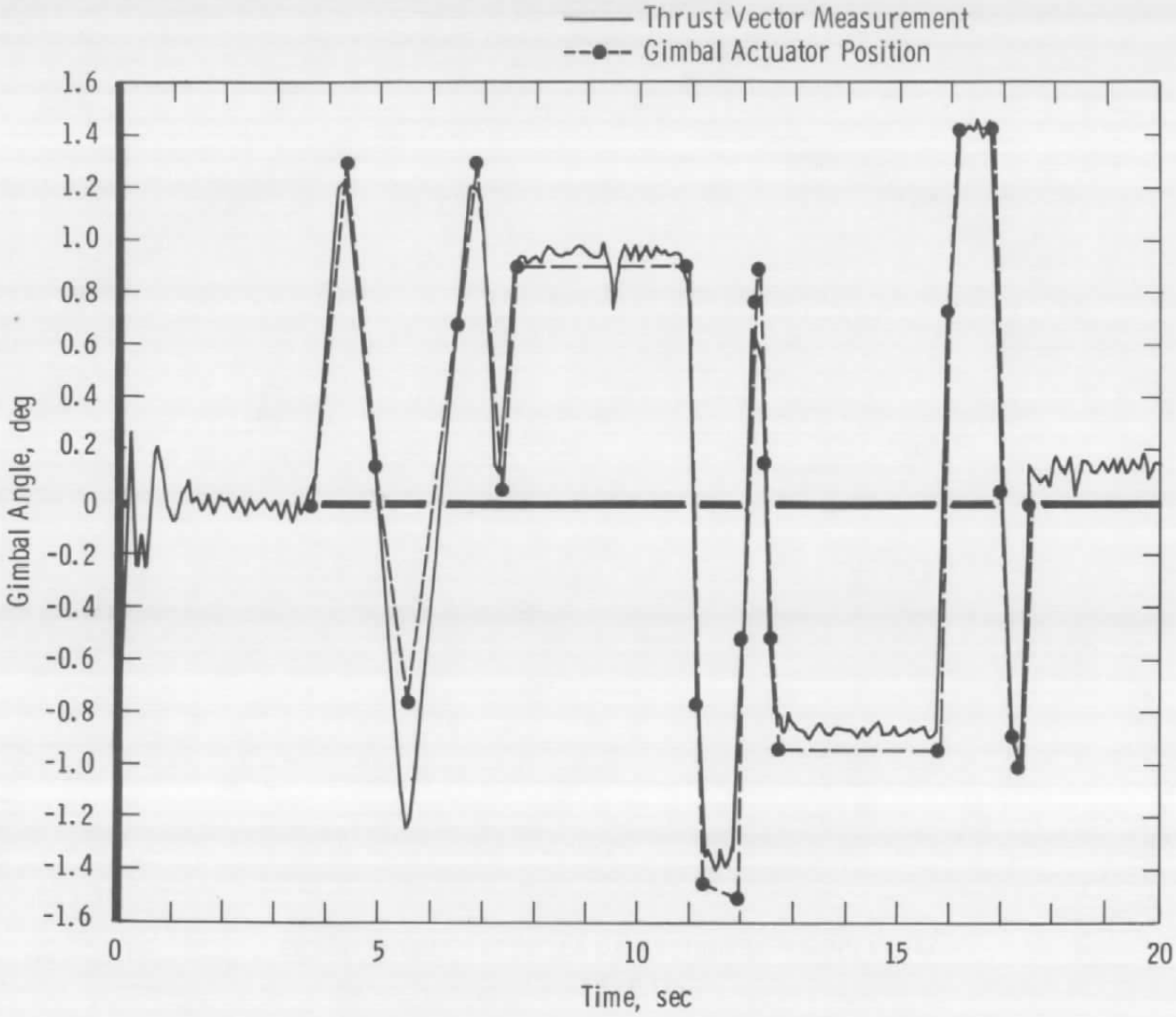

Fig. 13 Comparison of Actuator Position Indicator and Thrust Vector Calculations

TABLE I
ERROR IN REPEATABILITY OF CALIBRATION CONSTANTS

Calibration No.	F_{P_1}	$-F_{P_1}$	F_{Y_1}	$-F_{Y_1}$	F_a	F_R	$-F_R$	F_{P_2}	$-F_{P_2}$	F_{Y_2}	$-F_{Y_2}$
18A	0.96775	0.96241	0.98411	0.98117	0.99683	0.86513	0.86436	1.096	1.0968	1.0753	1.0636
18C	0.9669	0.96350	0.98173	0.97915	0.99733	0.86560	0.86961	1.0912	1.0918	1.0757	1.0753
20B	0.98535	0.9800	0.99499	0.99166	1.0004	0.92570	0.91223	1.0892	1.0328	1.0890	1.0906
20C	0.98549	0.98034	0.99317	0.99830	1.0007	0.91286	0.91265	1.0867	1.0535	1.0888	1.0897
23A	0.9857	0.98795	0.96555	0.96724	1.0130	0.91020	0.90834	1.0603	1.0745	1.0926	1.0762
23B	0.98941	0.98708	0.96582	0.96697	1.0115	0.91297	0.91007	1.0620	1.0550	1.0917	1.1447

TABLE II
PERCENTAGE CHANGE IN REPEATABILITY OF CALIBRATION CONSTANTS

Calibration No.	F_{P_1}	$-F_{P_1}$	F_{Y_1}	$-F_{Y_1}$	F_a	F_R	$-F_R$	F_{P_2}	$-F_{P_2}$	F_{Y_2}	$-F_{Y_2}$
18A-C	0.106	0.109	0.238	0.202	0.05	0.047	0.525	0.48	0.50	0.40	1.17
20B-C	0.014	0.034	0.182	0.064	0.03	1.28	0.042	0.05	2.07	0.02	0.09
23A-C	0.37	0.087	0.027	0.027	0.15	0.277	0.173	0.17	1.95	0.09	---

TABLE III

PERCENTAGE CHANGE OF CALIBRATION CONSTANTS OBTAINED DURING AXIAL CALIBRATIONS CONDUCTED AT AMBIENT AND SIMULATED ALTITUDE CONDITIONS

Calibration No.	Test Series	F_{P_1}	F_{P_2}	F_{Y_1}	F_{Y_2}	F_R
18A	G	0.363	0.363	1.56	0.10	---
19A	H	2.80	1.66	1.25	0.47	---
19	J	2.20	1.30	1.50	1.14	2.6
19	K	3.13	0	1.50	0.725	1.82
20C	L	0.835	1.66	0.73	1.14	1.30

TABLE IV

ONE STANDARD DEVIATION ACCURACY FOR INDIVIDUAL CALIBRATIONS

Calibration No.	F_{P_1}	$-F_{P_1}$	F_{Y_1}	$-F_{Y_1}$	F_a	F_R	$-F_R$	F_{P_2}	$-F_{P_2}$	F_{Y_2}	$-F_{Y_2}$
18A	0.156	0.296	0.464	0.406	0.06	0.635	1.78	0.98	0.450	0.101	0.276
18C	0.168	0.272	0.344	0.270	0.055	0.75	0.999	0.856	0.406	0.147	0.314
19A	0.11	0.10	0.706	0.775	0.189	1.56	1.83	1.36	0.320	0.208	0.526
19	0.27	0.66	0.361	0.302	0.051	0.42	0.213	0.376	0.084	0.150	0.298
20B	0.153	0.24	0.228	0.171	0.027	0.54	0.585	0.44	---	0.296	0.143
20C	0.205	0.376	0.240	0.223	0.034	0.437	0.54	0.348	1.08	0.244	0.308
21C	0.586	0.496	---	2.12	0.096	0.51	0.433	0.199	3.4	2.82	3.60
22A	0.986	0.758	1.62	0.876	0.018	1.058	0.207	0.394	1.78	0.49	0.412
23A	1.1	0.438	0.266	0.388	0.267	2.34	1.95	0.446	0.35	0.140	0.514
23B	1.096	0.460	0.195	0.446	0.124	0.128	0.11	0.54	1.16	---	---

TABLE V
LOAD CELL DESIGNATION

i	Data Load Cell Designation	
1	$F_{P_1\ data}$	(forward pitch)
2	$F_{Y_1\ data}$	(forward yaw)
3	$F_{a\ data}$	(axial)
4	$F_{R\ data}$	(roll)
5	$F_{P_2\ data}$	(aft pitch)
6	$F_{Y_2\ data}$	(aft yaw)

j	Calibrate Load Cell Designation	
1	$F_{P_1\ cal}$	(forward pitch)
2	$F_{Y_1\ cal}$	(forward yaw)
3	$F_{a\ cal}$	(axial)
4	$F_{R\ cal}$	(roll)
5	$F_{P_2\ cal}$	(aft pitch)
6	$F_{Y_2\ cal}$	(aft yaw)

z	Load Plane Designation
1	pitch plane
2	yaw plane
3	axial direction
4	roll direction

TABLE VI
ENGINE IDENTIFICATION

Chamber No.	Chamber S/N	Engine S/N	Test Series
1	47	11	G, H, J, K
2	77	9A	L

UNCLASSIFIED

Security Classification

DOCUMENT CONTROL DATA - R&D

(Security classification of title, body of abstract and indexing annotation must be entered when the overall report is classified)

1 ORIGINATING ACTIVITY (Corporate author) Arnold Engineering Development Center ARO, Inc. Operating Contractor Arnold Air Force Station, Tennessee	2a REPORT SECURITY CLASSIFICATION UNCLASSIFIED 2b GROUP N/A

3 REPORT TITLE

THRUST VECTOR DETERMINATION FOR THE APOLLO SERVICE PROPULSION ENGINE USING A SIX-COMPONENT FORCE BALANCE

4 DESCRIPTIVE NOTES (Type of report and inclusive dates)

N/A

5 AUTHOR(S) (Last name, first name, initial)

Robinson, C. E. and Runyan, R. B., ARO, Inc.

6 REPORT DATE	7a TOTAL NO OF PAGES	7b NO OF REFS
December 1965	48	1

8a CONTRACT OR GRANT NO	9a ORIGINATOR'S REPORT NUMBER(S)
AF 40(600)-1200 b System 921E c d	AEDC-TR-65-250 9b OTHER REPORT NO(S) (Any other numbers that may be assigned this report) N/A

10 AVAILABILITY/LIMITATION NOTICES

Qualified users may obtain copies of this report from DDC. Release to foreign governments or foreign nationals must have prior approval of AEDC.

11 SUPPLEMENTARY NOTES	12 SPONSORING MILITARY ACTIVITY
N/A	National Aeronautics and Space Administration Manned Spacecraft Center, Houston, Texas

13 ABSTRACT

A multicomponent force system was developed to determine the line of action of the forces generated by the Apollo Service Module engine. This force system was a force balance based on the principles of linear and repeatable installation tare effects. The basic concepts of the force balance and the statistical accuracies which were achieved are presented along with a detailed discussion of the calibration procedure and data reduction methods. Thrust vector excursion for two ablative combustion chambers during nongimbaling engine operation and limited thrust vector data during gimbaling operation are also presented. The precision of the thrust vector data was determined to be 0.033 deg for angular measurement and 0.026 in. for position determination.

DD FORM 1 JAN 64 1473

UNCLASSIFIED

Security Classification

14 KEY WORDS	LINK A		LINK B		LINK C	
	ROLE	WT	ROLE	WT	ROLE	WT
apollo service module engine						
force measurement systems						
six-component force balance						
thrust vector determination						
static testing						

INSTRUCTIONS

1. ORIGINATING ACTIVITY: Enter the name and address of the contractor, subcontractor, grantee, Department of Defense activity or other organization *(corporate author)* issuing the report.

2a. REPORT SECURITY CLASSIFICATION: Enter the overall security classification of the report. Indicate whether "Restricted Data" is included. Marking is to be in accordance with appropriate security regulations.

2b. GROUP: Automatic downgrading is specified in DoD Directive 5200.10 and Armed Forces Industrial Manual. Enter the group number. Also, when applicable, show that optional markings have been used for Group 3 and Group 4 as authorized.

3. REPORT TITLE: Enter the complete report title in all capital letters. Titles in all cases should be unclassified. If a meaningful title cannot be selected without classification, show title classification in all capitals in parenthesis immediately following the title.

4. DESCRIPTIVE NOTES: If appropriate, enter the type of report, e.g., interim, progress, summary, annual, or final. Give the inclusive dates when a specific reporting period is covered.

5. AUTHOR(S): Enter the name(s) of author(s) as shown on or in the report. Enter last name, first name, middle initial. If military, show rank and branch of service. The name of the principal author is an absolute minimum requirement.

6. REPORT DATE: Enter the date of the report as day, month, year, or month, year. If more than one date appears on the report, use date of publication.

7a. TOTAL NUMBER OF PAGES: The total page count should follow normal pagination procedures, i.e., enter the number of pages containing information.

7b. NUMBER OF REFERENCES: Enter the total number of references cited in the report.

8a. CONTRACT OR GRANT NUMBER: If appropriate, enter the applicable number of the contract or grant under which the report was written.

8b, 8c, & 8d. PROJECT NUMBER: Enter the appropriate military department identification, such as project number, subproject number, system numbers, task number, etc.

9a. ORIGINATOR'S REPORT NUMBER(S): Enter the official report number by which the document will be identified and controlled by the originating activity. This number must be unique to this report.

9b. OTHER REPORT NUMBER(S): If the report has been assigned any other report numbers *(either by the originator or by the sponsor)*, also enter this number(s).

10. AVAILABILITY/LIMITATION NOTICES: Enter any limitations on further dissemination of the report, other than those imposed by security classification, using standard statements such as:

(1) "Qualified requesters may obtain copies of this report from DDC."

(2) "Foreign announcement and dissemination of this report by DDC is not authorized."

(3) "U. S. Government agencies may obtain copies of this report directly from DDC. Other qualified DDC users shall request through _____."

(4) "U. S. military agencies may obtain copies of this report directly from DDC. Other qualified users shall request through _____."

(5) "All distribution of this report is controlled. Qualified DDC users shall request through _____."

If the report has been furnished to the Office of Technical Services, Department of Commerce, for sale to the public, indicate this fact and enter the price, if known.

11. SUPPLEMENTARY NOTES: Use for additional explanatory notes.

12. SPONSORING MILITARY ACTIVITY: Enter the name of the departmental project office or laboratory sponsoring *(paying for)* the research and development. Include address.

13. ABSTRACT: Enter an abstract giving a brief and factual summary of the document indicative of the report, even though it may also appear elsewhere in the body of the technical report. If additional space is required, a continuation sheet shall be attached.

It is highly desirable that the abstract of classified reports be unclassified. Each paragraph of the abstract shall end with an indication of the military security classification of the information in the paragraph, represented as *(TS), (S), (C), or (U)*

There is no limitation on the length of the abstract. However, the suggested length is from 150 to 225 words.

14. KEY WORDS: Key words are technically meaningful terms or short phrases that characterize a report and may be used as index entries for cataloging the report. Key words must be selected so that no security classification is required. Identifiers, such as equipment model designation, trade name, military project code name, geographic location, may be used as key words but will be followed by an indication of technical context. The assignment of links, rules, and weights is optional.